Coordination Chemistry Reviews 253 (2009) 1458–1475

Contents lists available at ScienceDirect

Coordination Chemistry Reviews

journal homepage: www.elsevier.com/locate/ccr

Review

Ligands and polymetallic complexes derived from 1,4-diformyl-2,3-dihydroxybenzene and two close analogues

Humphrey L.C. Feltham, Sally Brooker*

Department of Chemistry and the MacDiarmid Institute for Advanced Materials and Nanotechnology, University of Otago, PO Box 56, Dunedin, New Zealand

Contents

ARTICLE INFO

Article history:
Received 4 September 2008
Accepted 24 October 2008
Available online 5 November 2008

Keywords:
1,4-Diformyl-2,3-dihydroxybenzene
Polymetallic complexes
Imine
Oxime
Macrocycles
Acyclic ligands

ABSTRACT

Syntheses, structures and properties of polymetallic complexes prepared from both acyclic and cyclic ligands derived from the dialdehyde 1,4-diformyl-2,3-dihydroxybenzene (**1**), and two close analogues which also feature the 1,4-dicarbonyl-2,3-dihydroxy motif, are reviewed.

1. Introduction

1.1. Introductory remarks and scope of the review

Families of polymetallic complexes of acyclic and macrocyclic ligands derived from the dialdehyde "head unit" 1,4-diformyl-2,3-dihydroxybenzene (**1**) have been prepared and reported by the groups of Nabeshima and MacLachlan. This head unit provides two phenolate-bridging moieties, flanked by two aldehyde groups that are readily converted into imine or oxime groups thus providing additional donor atoms, so there is considerable potential for generating polymetallic complexes. Both the acyclic and macrocyclic ligands derived from **1**, and their metal complexes, are of interest due to their potential for use in a wide range of applications, including nano-machines, metal ion recognition, magnetism and supramolecular assemblies.

This review covers all compounds that are derived either from **1**, or from two very closely related analogues, 1,4-diformyl-2,3-dihydroxynaphthalene (**2**) and 1,4-dibenzoyl-2,3-dihydroxybenzene (**3**) (Fig. 1). To date the only 4,5-disubstituted

* Corresponding author. Tel.: +64 3 479 7919; fax: +64 3 479 7906.
E-mail address: sbrooker@chemistry.otago.ac.nz (S. Brooker).

0010-8545/$ – see front matter © 2008 Elsevier B.V. All rights reserved.
doi:10.1016/j.ccr.2008.10.017

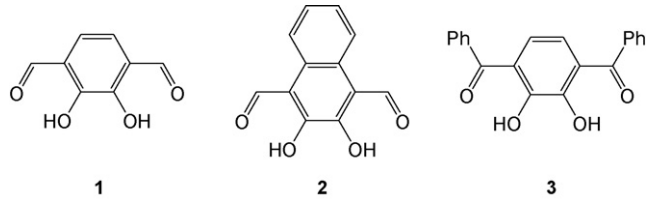

Fig. 1. The dialdehyde 1,4-diformyl-2,3-dihydroxybenzene (**1**) and the very closely related analogues 1,4-diformyl-2,3-dihydroxynaphthalene (**2**) and 1,4-dibenzoyl-2,3-dihydroxybenzene (**3**).

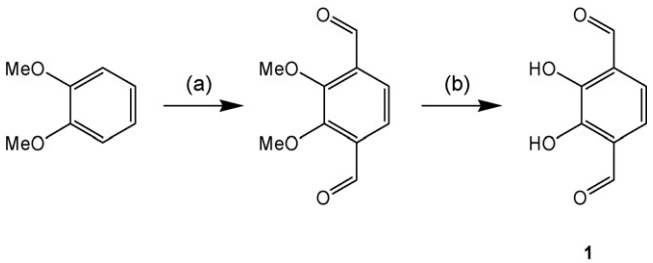

Fig. 2. Synthesis of **1** as published in Ref. [14]. Reagents and solvents: (a) (i) *n*-BuLi, TMEDA, Et_2O (ii) DMF (iii) H_2O and (b) (i) BBr_3, CH_2Cl_2 (ii) H_2O.

analogue of **1** is **2**, which is a special, rather than a general, case of 4,5-substitution as it features a fused ring. Compound **3** is the diphenylketone analogue of dialdehyde **1**. Ligands derived from **2** and **3** are included because they possess such a similar binding motif to the ligands derived from **1**. A variety of complexes of ligands derived from **1** have been reported, and will be discussed here. Complexes of ligands derived from 2 have only been mentioned in one instance; no *complexes* of ligands derived from **3** have been reported to date.

In addition to **2** and **3** there are many other precursors (to imine and oxime ligands) that are related, albeit less closely, to **1**. A brief overview of these is given in Section 1.3.

The first non-patent report of the use of **1** was by Nabeshima and co-workers: they communicated the preparation and structural characterisation of a metal-free [3 + 3] Schiff base macrocycle [1]. Independently, MacLachlan and co-workers had prepared a similar macrocycle which they reported [2]. These two groups remain the key players with regard to ligands and complexes derived from **1**.

Several patents that utilise **1** for processing photographic material have been lodged [3–11]. In addition, **1** has been used in the synthesis of an antibiotic [12] and in a study of hydrogen-bonded assemblies [13]. These are not detailed in this review as they do not fall into the area of interest, polymetallic coordination complexes, but references to them are provided for completeness.

1.2. Synthesis and reactions of *1*, *2* and *3*

The 2001 paper by Nabeshima and co-workers included the general method used to prepare **1**, but no experimental section

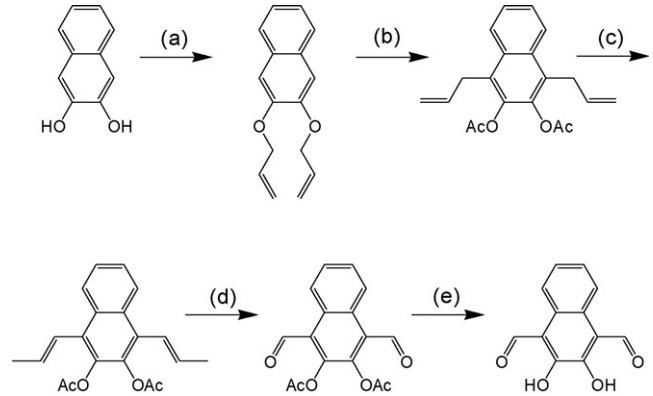

Fig. 3. Synthesis of **2** as published in Ref. [18]. Reagents and solvents: (a) 1-bromo-2-propene, K_2CO_3, acetone, (b) Δ, Et_3N, CH_2Cl_2, acetyl chloride, (c) $RhCl_3$, EtOH, THF (d) O_3, DMS, CH_2Cl_2 and (e) NaOH, MeOH, THF.

was provided. These details were published in 2006 (Fig. 2) [14]. In the interim, a synthetic procedure for the formylation of 1,2-dimethoxybenzene, the first step in the synthesis of **1**, was detailed by Kuhnert and co-workers [15].

Dialdehydes like **1** and **2**, in which the formyl group is conjugated to an aromatic ring, are particularly convenient precursors to Schiff bases because they react with primary amines in mild conditions, and demonstrate resilience to hydrolysis [16]. While several of the ligands derived from **1** are prepared in either warmed or refluxing solvent this is still mild: there have been no reports to date of needing to use acid catalysis or a drying agent to promote formation of the Schiff base bonds. The only ligands prepared to date from **2** did not require an acid catalyst or a drying agent, either [17,18].

The diketone **3** [19] can be condensed with a primary amine to generate robust ketimines that demonstrate particular stability. This permits the synthesis of ligands with two chemically distinct imine bonds, because once a suitable ketimine is prepared it can be reacted with a different aldehyde without fear of component exchange (see later, Figs. 21 and 22) [19].

Oximes (—CH=N—O—), which can be prepared by reaction of **1** with an alkoxy-substituted amine, also demonstrate good stability and can be used in a similar way to generate ligands with two different oxime bonds (see later, Fig. 8) [20].

The naphthalene analogue of **1**, 1,4-diformyl-2,3-dihydroxynaphthalene (**2**), was first reported in 1989 in a medicinal context [21]. Then in 1995 it was used by Reinhoudt and co-workers in the preparation of four Schiff base macrocycles [18] (see Section 3.1). That group synthesized **2** in five steps (Fig. 3) from commercially available 1,2-dihydroxynaphthalene.

The dialdehyde **2** has also been prepared using a different synthesis, by MacLachlan and co-workers. It was prepared by pyridinium chlorochromate (PCC) oxidation of the alcohol groups in 1,4-bis(hydroxymethyl)-2,3-dimethoxynaphthalene followed by deprotection of the methoxy groups to alcohols (Fig. 4) [17]. The diol 1,4-bis(hydroxymethyl)-2,3-dimethoxynaphthalene

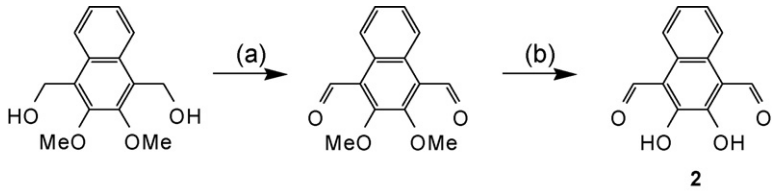

Fig. 4. Synthesis of **2** as published in Ref. [17]. Reagents and solvents: (a) PCC, $CHCl_3$, r.t., 2 h and (b) BBr_3, $CHCl_3$, r.t., 12 h.

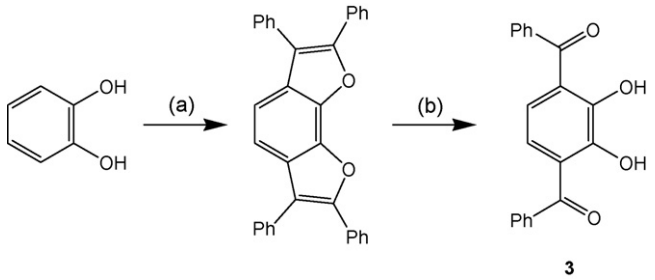

Fig. 5. Synthesis of **3** as published in Ref. [19]. Reagents and solvents: (a) benzoin, B_2O_3, 10 mins at 260 °C (b) (i) CrO_3, AcOH (ii) H_2SO_4.

is prepared from 1,2-dihydroxynaphthalene in three steps using a literature method [22].

The synthesis of the ketone **3** (Fig. 5) was reported by MacLachlan and co-workers [19].

Schiff base and oxime ligands derived from **1** have been used to prepare both *homometallic* and *heterometallic* complexes. The homometallic complexes are usually prepared by simply combining solutions of the metal ion and the ligand. In contrast, the heterometallic complexes have been prepared by two different methods. A combination of different metal ions in appropriate ratios can be added to a solution of the ligand, or alternatively, a homometallic complex can be formed first and then a transmetallation reaction can be used to introduce the different metal ion, whereby it displaces one (or more) of the original metal ions. The driving force for the transmetallation is usually the size, geometry preferences and/or charge of the incoming metal ion being better suited to the overall binding environment provided by the ligand than the original metal ion, leading to a more thermodynamically stable product [14,23,24].

1.3. Further analogues of *1*

Casting a wider net, the less-closely related analogues of **1** fall into two main groups. The first group consists of compounds which possess two carbonyl and two or four hydroxyl groups so at first glance look quite similar to **1**–**3** (Fig. 6). However, either the substitution pattern around the benzene ring is different, **4**, [19] and/or the compound contains additional functionality, specifically additional benzene rings; **5** [19], **6** [25] and **7** [26]. These have been used, by the groups of both Nabeshima and MacLachlan, exclusively in the preparation of macrocycles. MacLachlan and co-workers have prepared a number of large macrocycles for the purposes of investigating imine-keto/enamine tautomerization [17], synthesizing macrocycles with chemically inequivalent

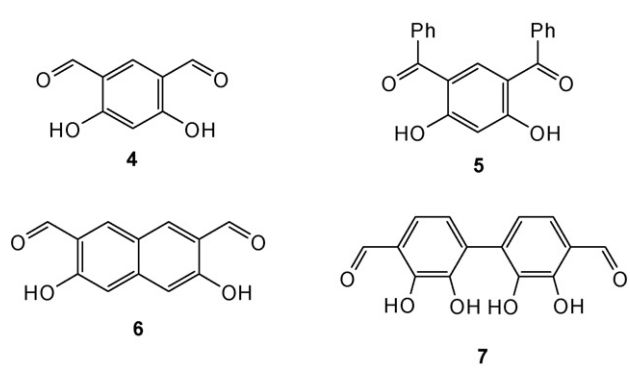

Fig. 6. A selection of analogues of **1** that have been used in the formation of macrocycles.

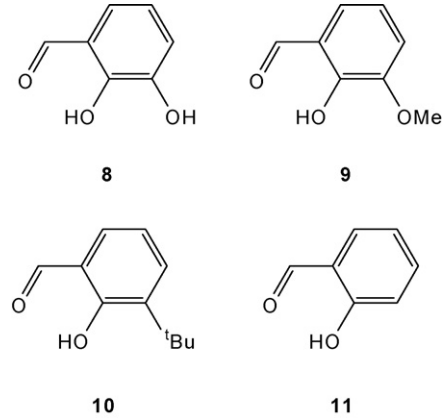

Fig. 7. Some mono-aldehyde and mono-hydroxyl analogues of **1** that have been reported in the literature.

imine bonds [19] or luminescent properties [27], and generating giant macrocycles (including the only example of a [6+6] Schiff base macrocycle) [25]. These macrocycles are also being investigated for their potential as receptors for organic molecules [17], and their coordination behaviour with metal ions is also being studied [19,25,27]. Nabeshima has reported a macrocycle with multiple hydroxyl groups as a potential system for binding organic molecules via hydrogen bonding [26]. To date, however, the coordination chemistry of these analogues is in its infancy. In contrast, the metal ion complexation reactions of macrocycles derived from **1** have been studied to a significant extent (Sections 2 and 3).

The second, much larger, group comprises compounds which are similar to **1** but lack either a formyl or a hydroxyl group or both. Only a small selection of such compounds is presented in Fig. 7. Of most interest in the context of the present review is the analogue of **1** in which one of the formyl groups is absent, 1-formyl-2,3-dihydroxybenzene (**8**), as this has been used by a number of research groups to create complexes ranging from simple mononuclear [28] systems to large octametallic Zn^{2+} [29], Co^{2+} [30] and U^{4+} [31] clusters. A large number of di- and trimetallic systems derived from **8** have also been characterised. In contrast, the metal complexes of *acyclic* ligands derived from **1** are exclusively tri- [14] or tetranuclear [23,32] (Section 2). In other cases one of the hydroxyl groups of **1** is replaced by a methoxy group, **9**, or a *t*Bu group, **10**. These two precursors have been used mainly in the preparation of acyclic ligands and a number of complexes have been reported. Salicylaldehyde (**11**), the commercially available analogue of **1** in which both one formyl and one hydroxyl group are absent, is such a well known ligand precursor that the number of complexes derived from it, including those involving the *salen* ligand, is vast.

2. Acyclic ligands and complexes

2.1. Synthesis of acyclic ligands from *1*

Nabeshima and co-workers have prepared five acyclic oxime ligands from **1** (Fig. 8). Because two different aldehydes are involved in the synthesis, oximes are used to prevent ligand component scrambling (which sometimes occurs with Schiff base ligands).

2.2. Homometallic complexes

Homometallic complexes were prepared by the reaction of $H_4\mathbf{L^1}$ [14], $H_4\mathbf{L^2}$ [14], $H_4\mathbf{L^3}$ [33] and $H_4\mathbf{L^4}$ with $Zn(OAc)_2{\cdot}2H_2O$. Treatment of $H_4\mathbf{L^1}$ or $H_4\mathbf{L^2}$ with three equivalents of $Zn(OAc)_2{\cdot}2H_2O$ in $EtOH/CHCl_3$ afforded the yellow *homotrimetallic* complexes

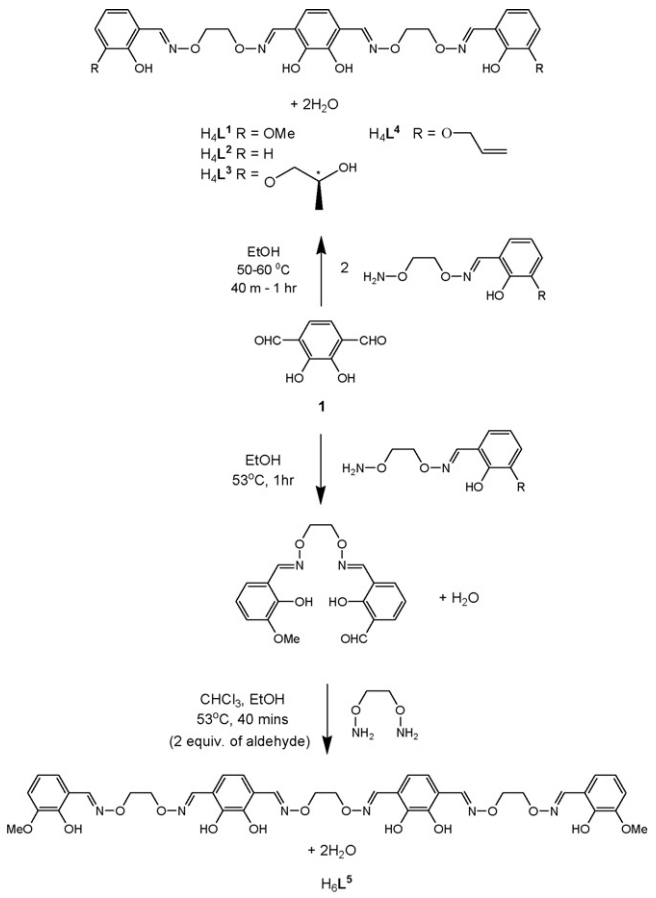

Fig. 8. Preparation of ligands $H_4\mathbf{L^1}$, $H_4\mathbf{L^2}$, $H_4\mathbf{L^3}$, $H_4\mathbf{L^4}$ and $H_4\mathbf{L^5}$ from **1**. No acid was used in the synthesis of these ligands. The chiral carbon atom in the R substituent of $H_4\mathbf{L^3}$ is shown here in the *S* configuration.

$[Zn_3(\mathbf{L^1})(OAc)_2]\cdot 3H_2O$ and $[Zn_3(\mathbf{L^2})(OAc)_2]\cdot 3H_2O\cdot Me_2CO$, in 82% and 52% yields following recrystallization, respectively [14]. The yellow complex $[Zn_3(\mathbf{L^4})(OAc)_2(MeOH)_2]\cdot 0.5CHCl_3$ was prepared by reaction of $Zn(OAc)_2\cdot 2H_2O$ in MeOH with $H_4\mathbf{L^4}$ in $CHCl_3$ in 73%, following recrystallization [34]. The analogous complex of $H_4\mathbf{L^3}$, $[Zn_2(\mathbf{L^3})(OAc)_2]$, has been prepared from $Zn(OAc)_2$, but no synthetic or structural details were provided [33].

Although no homometallic Zn^{2+} complex of $H_6\mathbf{L^5}$ could be isolated, ESI-MS of the reaction between $H_6\mathbf{L^5}$ and four equivalents of $Zn(OAc)_2$ showed a mixture of products—one of which was determined to be the *homotetrametallic* complex $[Zn_4(\mathbf{L^5})(OAc)_2]$ by virtue of a strong peak at the expected *m*/*z* [23].

The homometallic Zn^{2+} complexes were characterised by UV–vis spectroscopy [24], ^{1}H NMR spectroscopy, ESI mass spectrometry and X-ray crystallography. Upon coordination to the Zn^{2+} ions, the ligand undergoes an interesting conformational change. Rather than bridging two distant metal ions and forming a coordination polymer, as may be expected for a ligand of this length, the ligand curls into a 'C-shape' and binds three Zn^{2+} ions (Fig. 9). Two Zn^{2+} ions are bound in N_2O_2 pockets [14] and the third Zn^{2+} ion is bound to the deprotonated catechol oxygen donor atoms. Two slightly different crystal structures have been published for $[Zn_3(\mathbf{L^1})(OAc)_2(S)]$ which each contain a different coordinated solvent molecule (S), either ethanol [24] or water [14]. The structure where S = EtOH is shown in Fig. 8.

Three further *homotrimetallic* complexes of first-row transition metal ions were prepared by Nabeshima and co-workers, and characterised by ESI-MS, absorbance spectroscopy and X-ray crystallography. Addition of three equivalents of $Mn(OAc)_2\cdot 4H_2O$ in MeOH to a solution of $H_4\mathbf{L^1}$ in $CHCl_3$/MeOH resulted in the corresponding *homotrimetallic* complex $[Mn^{II}{}_3(\mathbf{L^1})(OAc)_2]\cdot 2MeOH$, in 72% yield following recrystallization [35]. Likewise, the complexation of $Co(OAc)_2\cdot 4H_2O$ in EtOH with $H_4\mathbf{L^1}$ in $CHCl_3$/EtOH produced the analogous *homotrimetallic* complex $[Co^{II}{}_3(\mathbf{L^1})(OAc)_2]\cdot 0.5EtOH.1\cdot 5H_2O\cdot CHCl_3$, in 64% yield following recrystallization [35]. The analogous *homotrimetallic* nickel(II) complex with the formula $[Ni^{II}{}_3(\mathbf{L^1})(OAc)_2]\cdot 2MeOH\cdot 3H_2O$ was prepared in CH_2Cl_2 in 68% yield [35], although no crystal struc-

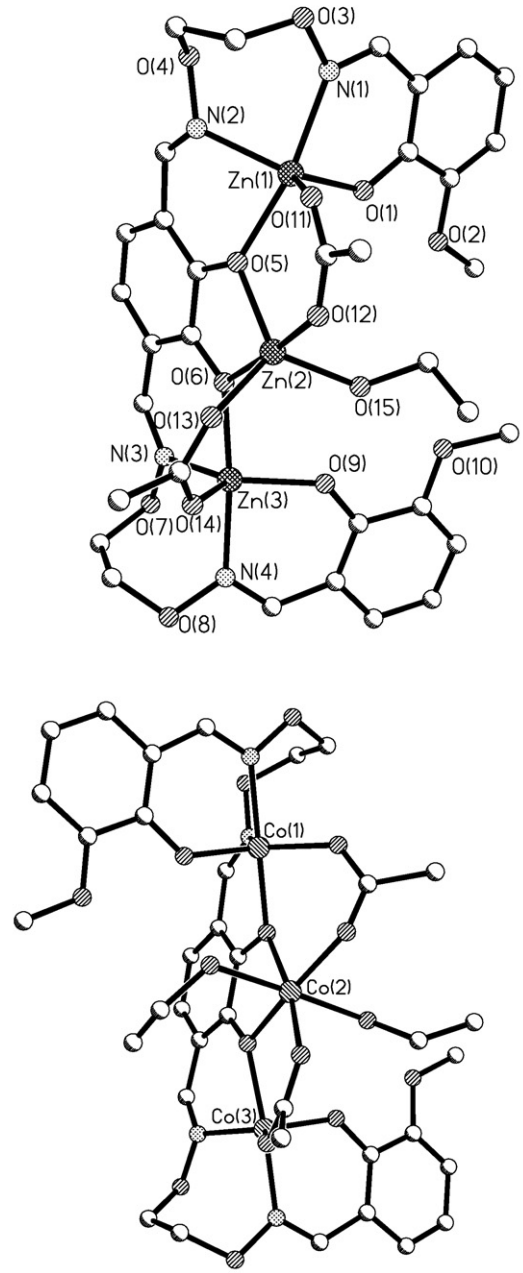

Fig. 9. Crystal structure of $[Zn_3(\mathbf{L^1})(OAc)_2(EtOH)]$ (top) and $[Co^{II}{}_3(\mathbf{L^1})(OAc)_2(EtOH)_2]$ (bottom). For clarity, solvent molecules, hydrogen atoms and disordered atoms have been omitted. This figure was generated from data obtained from the Cambridge Crystallographic Data Centre as published originally in Refs. [23,35].

ture was reported. The crystal structures of the Mn^{II}_3 and Co^{II}_3 complexes contained two coordinated alcohol solvent molecules each (MeOH for Mn^{II}_3 and EtOH for Co^{II}_3). The Co^{II}_3 complex is interesting because in the crystal state coordination of the cobalt ions to $(\mathbf{L^1})^{4-}$ conforms the ligand into an 'S-shape' (Fig. 9), rather than the 'C-shape' seen in other similar homometallic complexes of the ligand. The complex $[Zn_3(\mathbf{L^4})(OAc)_2]$ is also S-, rather than C-shaped. Attempts to form a tricopper complex were unsuccessful and ESI-MS indicated that mono- and dicopper species had been formed. The researchers argue that the Cu^{2+} ions in the N_2O_2 pockets are not prone to coordinate an acetate ligand axially and thus a strong interaction with the third Cu^{2+} ion is less favoured. This hypothesis was reinforced by an experiment in which $H_4\mathbf{L^1}$ was reacted with metal *chlorides* of Mn^{2+}, Co^{2+} and Ni^{2+}. ESI-MS showed the presence of dimetallic species but trimetallic complexes were not forming to any great extent. This suggests that the acetate ion is an essential component of the reaction for forming trimetallic species cooperatively.

2.3. Heterometallic complexes

$[Zn_3(\mathbf{L^1})(OAc)_2(S)]$ can be converted into a large family of heterometallic analogues with the general formula $[Zn_2M^{III}(\mathbf{L^1})(OAc)_3]\cdot$solvent or $[Zn_2M^{II}(\mathbf{L^1})(OAc)_2]\cdot$solvent by transmetallation with the acetate salt of the appropriate metal ion. There are three reported exceptions to these general formulae. Firstly, the group three heterometallic complexes are prepared by transmetallation with nitrate salts (rather than acetates) and as a result the complexes contain nitrate ions; coordinated in the case of $[Zn_2Y(\mathbf{L^1})(OAc)_2(NO_3)]$ and as a closely associated counter-anion in the cationic complex $[Zn_2Sc(\mathbf{L^1})(OAc)_2](NO_3)$. Secondly, the heterotrimetallic $[Zn_2Eu(\mathbf{L^1})(OAc)_2(NO_3)(H_2O)]$ complex was also prepared by transmetallation with the nitrate salt rather than the acetate salt. Thirdly, the complex $[Zn_2Ca(\mathbf{L^1})(ClO_4)_2(MeOH)_2]$ contains two coordinated perchlorate ions. In all cases the incoming metal ion displaces one Zn^{2+} ion from the central O_6 binding site (Fig. 10). As an alternative to this transmetallation route (Fig. 10, top route) a one-pot approach can also be taken (Fig. 10, bottom route).

The transmetallation reaction was originally performed with Eu^{3+} [24]. Subsequently it has been reported [14] that all lanthanide ions (from La^{3+} to Lu^{3+}) and some group two (Ca^{2+}, Sr^{2+} and Ba^{2+}) and group three (Sc^{3+}, Y^{3+}) metal ions will also displace the central Zn^{2+} ion. The creation of the heterotrimetallic complexes was generally confirmed by microanalysis and X-ray diffraction of a single crystal of the complex. In some cases changes in the UV–vis spectrum of the homometallic complex as the new metal ion was introduced was used as evidence [14,24]. All of the heterometallic complexes are yellow, as is $[Zn_3(\mathbf{L^1})(OAc)_2(S)]$, and the yield varied depending on the central metal ion—between 68% (Dy^{3+}) and 92% (Nd^{3+}).

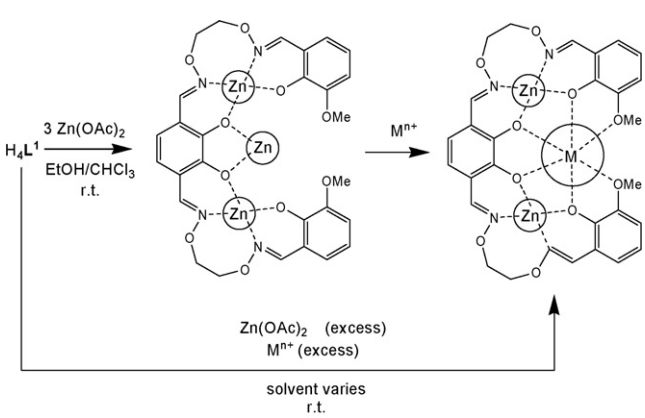

Fig. 10. Different synthetic routes to heterometallic complexes of $H_4\mathbf{L^1}$ using zinc(II) acetate and a generalized metal ion. For clarity, any coordinated acetate, water, methanol/ethanol, nitrate or perchlorate molecules have been omitted.

The one-pot approach also provided access to a heterotrimetallic complex of Cu^{2+} and Gd^{3+} ions [36]. The dark brown heterometallic complex $[Cu^{II}_2Gd(\mathbf{L^1})(OAc)_3]$ was prepared in 79% yield by addition of two equivalents of $Cu(OAc)_2\cdot H_2O$ in EtOH and one equivalent of $Gd(OAc)_3\cdot 4H_2O$ in $MeOH/H_2O$ to a solution of $H_4\mathbf{L^1}$ in $EtOH/CHCl_3$. The transmetallation route described above for the trizinc complex could not be taken in this case as the analogous tricopper complex $[Cu_3(\mathbf{L^1})(OAc)_2]$, could not be isolated.

In a later report, Nabeshima and co-workers prepared two heterotrimetallic complexes of the ligand $H_4\mathbf{L^1}$ by the one-pot approach in which all three metal ions were first-row transition metal ions [35]. The complex $[Zn_2Mn^{II}(\mathbf{L^1})(OAc)_2]\cdot MeOH\cdot H_2O$ was synthesized in 95% yield by the addition of one equivalent of $Mn(OAc)_2\cdot 2H_2O$ in MeOH and two equivalents $Zn(OAc)_2\cdot 2H_2O$ in MeOH to a solution of one equivalent of $H_4\mathbf{L^1}$ in $CHCl_3$. The complex $[Cu^{II}_2Zn(\mathbf{L^1})(OAc)_2]\cdot 2H_2O$ was synthesized in an analogous manner in 91% yield using two equivalents of $Cu(OAc)_2\cdot H_2O$ instead of $Mn(OAc)_2\cdot 4H_2O$. In these complexes the two Zn^{2+} or two Cu^{2+} ions occupy the two outer N_2O_2 binding pockets, while the lone Mn^{2+} or Zn^{2+} ion occupies the central O_6 site.

ESI-MS was used to tentatively identify the predominant complex formed from reaction of $H_4\mathbf{L^1}$ with three equivalents of one transition metal (II) ion and three equivalents of a different transition metal (II) ion. Heterotrimetallic complexes of formula $[M^{II}_2Mn^{II}(\mathbf{L^1})]^{2+}$ were the main species formed in solutions where one of the metal ions is Mn^{II} and the other, M^{II}, is Co^{II}, Ni^{II} or Cu^{II}. When one of the metal ions is Cu^{II} and the other is either $M^{II} = Ni^{II}$ or Mn^{II}, the ESI-MS data is consistent with the presence of the heterotrimetallic complex $[Cu^{II}_2M^{II}(L^1)]^{2+}$, in which the Cu^{II} ions presumably occupy the outer N_2O_2 pockets. Other metal ion combinations, Cu^{2+}/Co^{2+}, Co^{2+}/Ni^{2+} and Ni^{2+}/Zn^{2+}, produced a greater variety of species, including di-, tri- and tetrametallic, and both homo- and heterometallic, complexes. None of these complexes, tentatively identified by ESI-MS, were isolated.

Formation of the heterotrimetallic complexes depends on the suitability of the incoming metal ion. Lanthanide ions have a larger ionic radius than Zn^{2+} and may form six, instead of two, coordination bonds between the central metal ion and $(\mathbf{L^1})^{4-}$ because, unlike the smaller ions, they are large enough to coordinate to the two methoxy groups of $(\mathbf{L^1})^{4-}$. The charge of the metal ion is also important. Trivalent lanthanide ions interact more strongly with the negatively charged phenolate oxygens than divalent zinc ions can, while monovalent cations interact weakest of them all. Both suitable charge and ionic radius are likely required to make the desired heterometallic complex more thermodynamically stable than the homometallic complex. For this reason, Na^+, K^+, Rb^+ and Cs^+ could not displace the central Zn^{2+} ion from $[Zn_3(\mathbf{L^1})(OAc)_2]$ [14,23], whereas lanthanide ions result in conversion to the heterometallic complex in reasonable to high yield [14]. This selectivity can potentially be utilized to model selective ion recognition in biological systems. When exposed to a range of physiologically important metal ions such as Na^+, K^+, Ca^{2+} and Mg^{2+}, $[Zn_3(\mathbf{L^1})(OAc)_2]$ transmetallated with Ca^{2+} to a far greater extent, by virtue of its appropriate size for the cavity and 2^+ charge [23]. The preference for Ca^{2+} over other metal ions provides a potential model for selective ion recognition in biologically important processes such as neuronal function in the hippocampus [14,23].

The importance of the two additional coordination bonds in stabilizing the heterometallic complex over the homometallic complex was reinforced by an experiment investigating the effect of

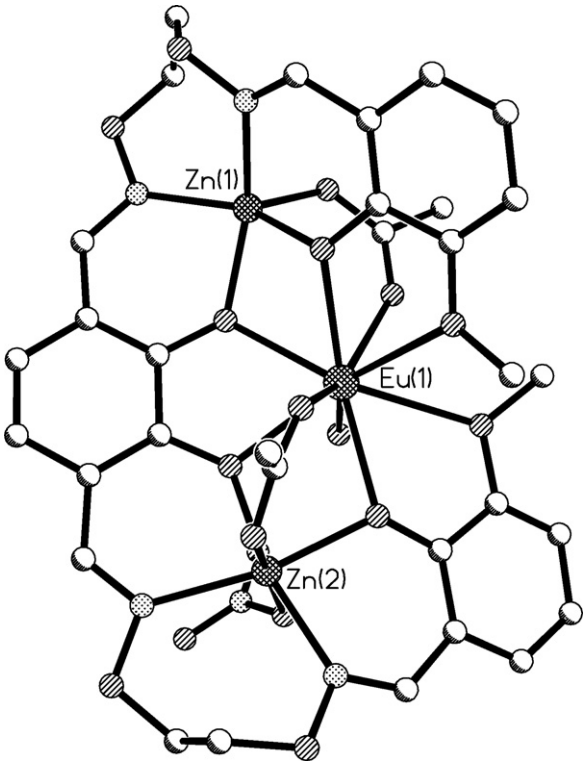

Fig. 11. Crystal structure of $[Zn_2Eu(\mathbf{L^1})(OAc)_2(NO_3)(H_2O)]$. This figure was generated from data obtained from the Cambridge Crystallographic Data Centre as published originally in Ref. [24]. For clarity, hydrogen atoms and solvent molecules have been omitted.

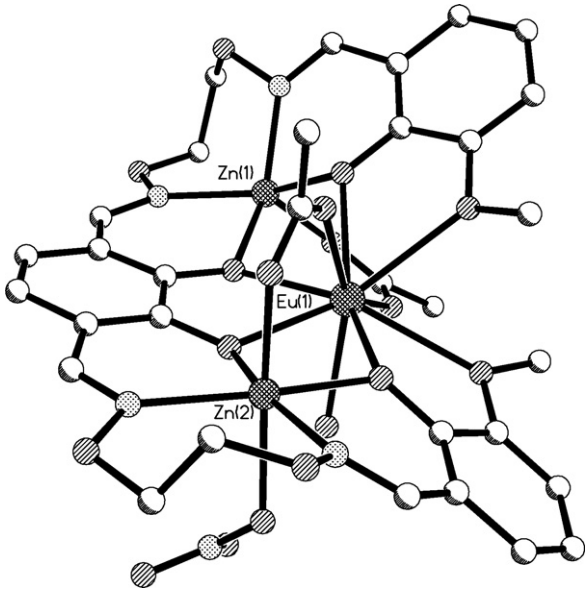

Fig. 12. Another view of the crystal structure of $[Zn_2Eu(\mathbf{L^1})(OAc)_2(NO_3)(H_2O)]$ from a perspective showing the helical conformation which is typical of the heterotrimetallic complexes. This figure was generated from data obtained from the Cambridge Crystallographic Data Centre as published originally in Ref. [24].

ligand substitution on complexation. The ligand $H_4\mathbf{L^2}$ is an analogue of $H_4\mathbf{L^1}$ that has hydrogen atoms in place of the methoxy substituents and hence provides only four, not six, oxygen donors to the central metal ion. The homometallic complex $[Zn_3(\mathbf{L^2})(OAc)_2]$ (Section 2.2) could not be transmetallated. This is consistent with the proposal that the increased stability generated by two additional coordination bonds is a significant factor in favouring the heterometallic complex over the homometallic analogue [14].

The acetate ions are indispensable for the formation of both the homo- and heterometallic complexes. The reaction of $H_4\mathbf{L^1}$ with $Zn(NO_3)_2$ and $Eu(NO_3)_3$ yielded no complex. However, the heterometallic complex was produced upon the addition of six equivalents of KOAc—four to deprotonate the hydroxyl groups and two as bridging ligands. Acetate ions are commonly used to aid in deprotonation of the ligands and, by bridging the metal ions, likely stabilize the molecule.

The heterometallic Zn^{2+}/M^{n+} complexes are helical (X-ray) (Figs. 11 and 12), a conformation templated by the central metal ion. The 'winding-angle' of the helix – that is, how tightly it wraps around the central metal ion – could be tuned by using different sized metal ions. In this way, the complex is a potential 'molecular spring or coil' [14]. If a chiral centre is introduced into the ligand, then diastereoisomeric forms of the helix can be created. Specifically, the heterometallic complex $[Zn_2Ca(\mathbf{L^3})(OAc)_2]$, prepared by the transmetallation of $[Zn_3(\mathbf{L^3})(OAc)_2]$ with two equivalents of $Ca(ClO_4)_2$, rather than $Ca(OAc)_2$, exists in two diastereoisomeric forms at low temperature [33]. There is no crystal structure and thus the details of coordinated solvent molecules were not reported, although it is speculated that the structure may be similar to the $\mathbf{L^1}$ analogue. Below 253 K, the thermodynamic barrier to conversion between the diastereoisomers becomes appreciable, such that in the ^{1}H NMR spectrum at 223 K, well-defined resonances are seen for the protons of both diastereoisomers. As the temperature is raised the separate signals begin to coalesce and at 253 K the two forms interconvert rapidly enough on the NMR timescale that an averaged signal is observed for each proton. The ratio of right-handed:left-handed forms, which can be observed when the temperature is low enough to prevent interconversion, is dependent on the difference in the thermodynamic stabilities of the diastereoisomers. For Ca^{2+}, Y^{3+} and La^{3+} the ratios were 80:20, 56:44 and 53:47 for right- and left-handed forms, respectively. Thus the complex $[Zn_2Ca(\mathbf{L^3})(OAc)_2]$ possesses the largest difference in thermodynamic stability between its two diastereoisomers. The dependence of the relative stabilities of the diastereomers on the choice of metal ion is believed to be the result of non-covalent interactions between the pendant 2-hydroxylpropyl groups, the strength of which is tuned by the winding angle of the helix. Molecular helicies are of interest because they can potentially form functional supramolecular materials, as well as contribute to knowledge of self-assembly and molecular recognition processes [37].

The acyclic ligand $H_4\mathbf{L^4}$ (Fig. 8), synthesized from **1**, can be cyclized by treatment with a Grubbs catalyst. The resulting double bond has either a *cis* (*Z*) or *trans* (*E*) configuration (Fig. 13). The isomer formed was dependent on whether or not metal ions were

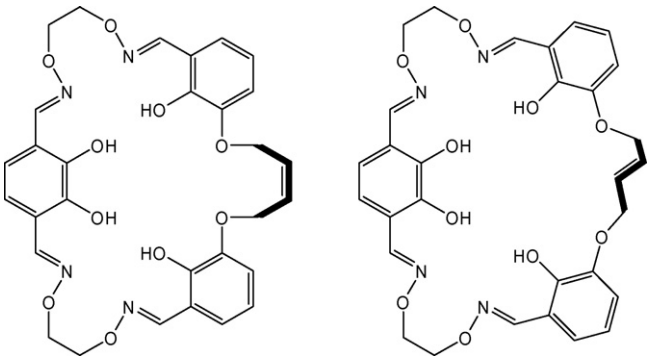

Fig. 13. The *cis*-closure of $H_4\mathbf{L^4}$ (*left*) compared with the *trans*-closure.

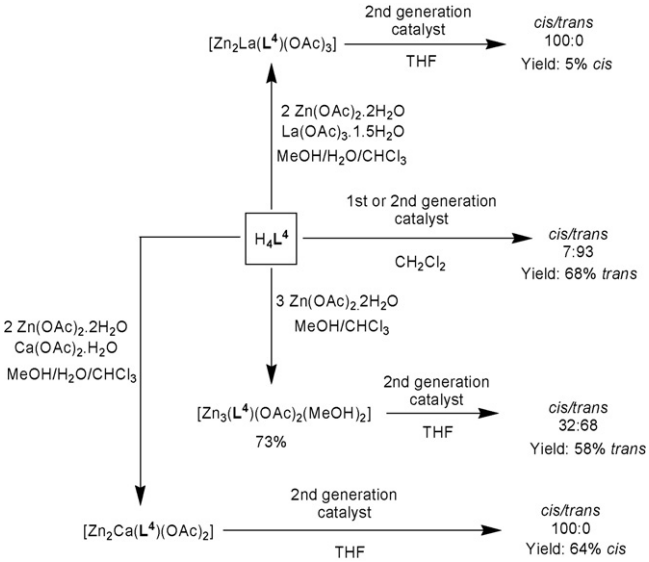

Fig. 14. Overview of potential cyclization methods for $H_4\mathbf{L^4}$.

coordinated to the ligand and, if so, the type of metal ions (Fig. 14) [34]. If the free ligand is treated with a first or second generation Grubbs catalyst, the product of the ring closure is almost exclusively *trans* (*cis*/*trans* ratio of 7:93). If the trimetallic zinc complex of $H_4\mathbf{L^4}$, $[Zn_3(\mathbf{L^4})(OAc)_2(MeOH)_2]$, is treated with a second generation Grubbs catalyst, then the ratio of isomers in the product mixture is 32:68 *cis*:*trans* following demetallation with HCl. If either of the two heterometallic complexes $[Zn_2Ca(\mathbf{L^4})(OAc)_2]\cdot 0.5H_2O$ or $[Zn_2La(\mathbf{L^4})(OAc)_3]0.5CHCl_3$, prepared in 80% and 88% yield, are subsequently treated with a second generation catalyst, then the resulting macrocycle is entirely *cis* following demetallation.

However, it should be stressed that the isomer ratios reported here do not necessarily reflect the actual yield of either macrocycle isomer (Fig. 14). For instance, despite exclusive formation of the *cis*-macrocycle from the ring closure of $[Zn_2Ca(\mathbf{L^4})(OAc)_2]$, the yield is only 64%. In the case of $[Zn_2La(\mathbf{L^4})(OAc)_3]$, the yield of the *cis*-macrocycle is only 5%, due to the formation of mono- and bis-deallylated products. The yield of the *trans* macrocycle from the closure of $[Zn_3(\mathbf{L^4})(OAc)_2(MeOH)_2]$ was 58%.

The ligand $H_6\mathbf{L^5}$ (Fig. 8) has been used to create two neutral helices incorporating four metal ions each [32] three in the strand itself and a fourth central one which templates the helical structure. As described above, addition of $Zn(OAc)_2$ to $H_6\mathbf{L^5}$ formed a mixture of complexes including the desired homometallic precursor $[Zn_4(\mathbf{L^5})(OAc)_2]$ [23]. In contrast to $[Zn_3(\mathbf{L^1})(OAc)_2]$, $[Zn_4(\mathbf{L^5})(OAc)_2]$ could not be transmetallated with Ca^{2+} (or K^+, Cs^+ and Mg^{2+}) because the central cavity is too large. Addition of one equivalent of Ba^{2+} to this mixture gave a simple, sharp ^1H NMR spectrum consistent with the formation of the just the yellowish-orange complex $[Zn_3Ba(\mathbf{L^5})(OAc)_2]$. Thus, the reaction of $Zn(OAc)_2$ with $H_6\mathbf{L^5}$ gives a product mixture that serves as a selective receptor for Ba^{2+} [23]. This complex could also be prepared by a one-pot reaction and, likewise, the reaction of $H_6\mathbf{L^5}$ with three equivalents of Zn^{2+} and one of La^{3+} produced the heterometallic complex $[Zn_3La(\mathbf{L^5})(OAc)_3]$ in almost quantitative yield. The central metal ion was again found to influence the movement of the helix. Interconversion between the left- and right-handed forms of the helix results in expansion and contraction of the molecule along the axis running up through the helix, a process which was studied by ^1H NMR. At 353 K, the ^1H NMR spectrum of $[Zn_3Ba(\mathbf{L^5})(OAc)_2]$ gave coalesced signals indicative of rapid inversion between the left- and right-handed forms. At the same temperature, the ^1H NMR spectrum of $[Zn_3La(\mathbf{L^5})(OAc)_3]$ gave sharp, distinct signals for the two different forms. Thus, the inversion was faster when Ba^{2+} was coordinated than when La^{3+} was. Three possible reasons for this have been proposed: (a) the coordination bonds in $[Zn_3Ba(\mathbf{L^5})(OAc)_2]$ are easier to break because Ba^{2+} is divalent and interacts less strongly with the phenolate oxygens of the helix than La^{3+} does (b) Ba^{2+} also has a larger ionic radius and forms a looser helix with a larger winding angle. (c) The three acetate ions in $[Zn_3La(\mathbf{L^5})(OAc)_3]$ more securely fix the conformation of the helix than the two acetate ions in $[Zn_3Ba(\mathbf{L^5})(OAc)_2]$ can [32].

3. Macrocyclic ligands and complexes

3.1. Synthesis of macrocycles from *1*, *2* and *3*

The first macrocycle based on **1**, $H_6\mathbf{L^6}$ (Fig. 15), was reported by Nabeshima and co-workers and is an example of a hydrogen-bonded, salen-like [3 + 3] Schiff base macrocycle [1]. Very few [3 + 3] macrocycles have been reported in the literature (the earliest examples were reported in the period 1987–1993 and involve 2,6-diformylphenol head units, see Refs. [38–41]), as [1 + 1] and [2 + 2] macrocycles are far more common [42].

Interestingly, $H_6\mathbf{L^6}$ was formed in the absence of a metal template ion in excellent yield, 91%. Direct macrocycle synthesis can often lead to the formation of undesired macrocycles and polymers [43,44]. Here, however, the [3 + 3] macrocycle is selectively formed because the oligomeric intermediates leading to $H_6\mathbf{L^6}$ are held in a favourable conformation by hydrogen bonding [1]. Additionally, the reversibility of imine bond formation allows thermodynamically favoured products to form over kinetic ones. The low solubility of $H_6\mathbf{L^6}$ is also considered to be an important driving force in its formation because pure macrocycle is gradually precipitated during the reaction, driving the equilibrium towards $H_6\mathbf{L^6}$ [1,43].

Crystals of $H_6\mathbf{L^6}$ with differing solvation, $H_6\mathbf{L^6}\cdot H_2O\cdot MeCN$ and $H_6\mathbf{L^6}\cdot 3MeCN$, were obtained and the structures determined (Fig. 16). In both structures each catechol oxygen atom is hydrogen bonded to the nitrogen atom of the adjacent imine bond and the catechol units are twisted out of the plane of the macrocycle (by about 30° in $H_6\mathbf{L^6}\cdot 3MeCN$) to reduce electrostatic repulsion between the hydroxyl groups (Fig. 16). The key difference between the structures is that in $H_6\mathbf{L^6}\cdot H_2O\cdot MeCN$ the hydroxyl groups all point towards the same face of the macrocycle (there are two bifurcated hydrogen bonds between four hydroxyl groups and a central water molecule) while in $H_6\mathbf{L^6}\cdot 3MeCN$ four hydroxyl groups point to one face but the remaining two point the other way [1].

Independently, MacLachlan and co-workers had prepared related [3 + 3] macrocycles $H_6\mathbf{L^7}$ (Fig. 17) with greater solubility than $H_6\mathbf{L^6}$ thanks to hydrophobic alkoxy chains of varying length on the diamine. The first such macrocycle [2], possessing $R = C_6H_{13}$ chains, was reported in 2003 by MacLachlan and co-workers and

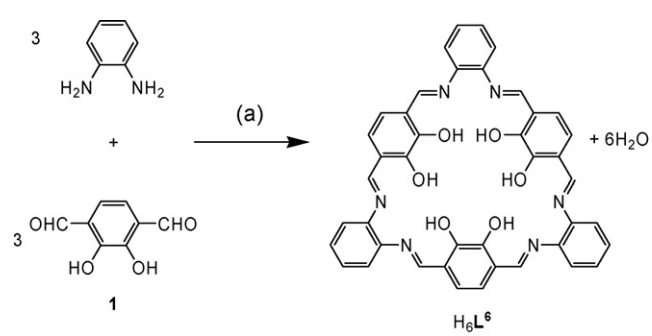

Fig. 15. Preparation of $H_6\mathbf{L^6}$ from **1**. Solvents and conditions: (a) MeCN, r.t., 2 weeks.

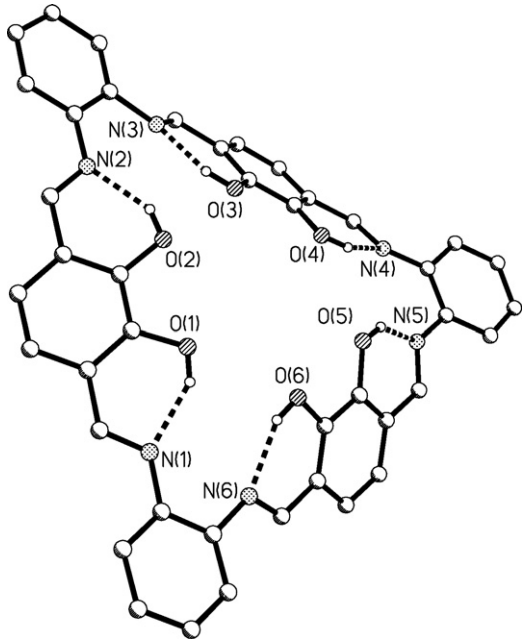

Fig. 16. Crystal structure of $H_6\mathbf{L^6}\cdot H_2O\cdot MeCN$. All of the catechol hydroxyl groups all point to the same face of the macrocycle. For clarity, solvent molecules and hydrogen atoms have been omitted. Dotted lines indicate hydrogen bonds.

was soluble in a range of organic solvents such as toluene and chloroform. Published crystal structures show that, excluding the alkoxy chains, the general features of $H_6\mathbf{L^7}$ in the solid state are similar to those in $H_6\mathbf{L^6}$. They found that other variants of $H_6\mathbf{L^7}$ were soluble enough to be purified as long as the alkyl chains were at least two carbon atoms long [45]. Macrocycles with chain lengths ranging between one and sixteen carbon atoms long have since been prepared by MacLachlan [45] and Nabeshima [46,47]. As with $H_6\mathbf{L^6}$, $H_6\mathbf{L^7}$ is synthesized without a metal template, although macrocycles with long alkoxy chains ($R = C_8H_{17}$ or longer) take longer to synthesize than those with shorter chains. This may be due to aggregation of the diamine starting material (which has the alkoxy chains) in the solvent.

MacLachlan and co-workers were also successful in creating an unsymmetrical analogue of $H_6\mathbf{L^7}$, in which one of the six imine bonds is reduced to an amino group (i.e. —CH=N— to —CH_2—NH—) in $CHCl_3$ without the addition of any formal reducing agent [48]. The formation of the red, mono-reduced macrocycle was explained through the formation of a 1:1 condensation by-product that is able to act as a reductant (reduces the macrocycle *in situ*), thereby oxidizing itself into an aromatic and stable species (Fig. 18). The stable

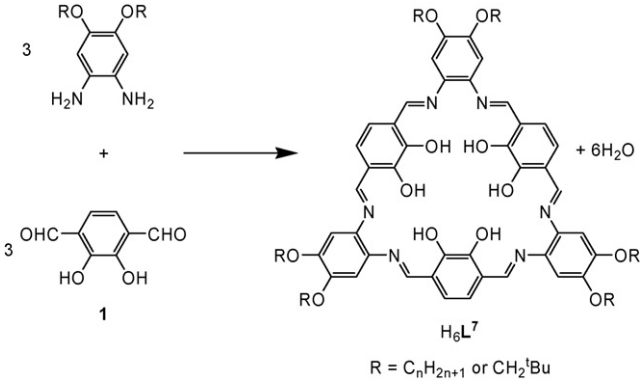

Fig. 17. Preparation of $H_6\mathbf{L^7}$. Solvents and conditions vary.

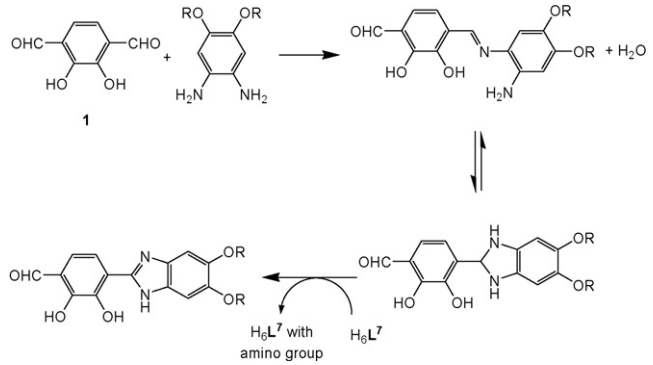

Fig. 18. MacLachlan mechanism for *in situ* reduction of one out of six imine bonds of $H_6\mathbf{L^7}$. $R = C_4H_9$, C_5H_{11} or C_6H_{13}.

by-product, as well as the fact that $H_6\mathbf{L^7}$ is not aromatic (48 π electrons) and therefore reduction does not break aromaticity, were the suggested driving forces for the partial reduction. Additionally, the reduction was only successful when commercial chloroform was used—the reduced macrocycle could not be produced in acid-free chloroform. Furthermore, the reduction in commercial $CHCl_3$ was significantly faster if a small amount of acid was added. The reduction of $H_6\mathbf{L^7}$ was successful for alkoxy chain lengths of $R = C_4H_9$, C_5H_{11} and C_6H_{13} in yields 53%, ~50% and 47%, respectively, following recrystallization from $CHCl_3$/MeCN. It is not mentioned whether reduction of macrocycles with other substituents was attempted, although judging from the three exemplars the length of the chain does not appear to affect the reaction. The group did not discover how to proceed past mono-reduction of $H_6\mathbf{L^7}$ without a formal reducing agent, and no other authors have reported a partially reduced macrocycle.

The Nabeshima group has also investigated multi-metal-ion templated formation of a different [3 + 3] macrocycle, $H_6\mathbf{L^8}$, based on **1** (Fig. 19) [43]. The addition of $Zn(OAc)_2$ (3 equiv.) and $La(OAc)_3$ (1 equiv.) to a solution of **1** (3 equiv.) in MeOH/$CHCl_3$ resulted in a non-macrocyclic planar intermediate complex, the structure of which was determined by mass spectrometry and X-ray crystallography. One La^{3+} ion and three Zn^{2+} ions aggregate three molecules

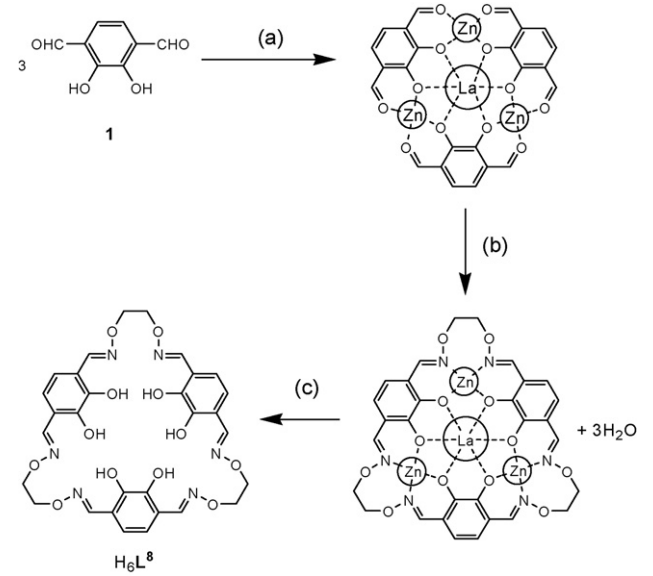

Fig. 19. Preparation of $H_6\mathbf{L^8}$. In the intermediate, coordinated methanol and nitrate molecules, as well as solvent molecules have been omitted for clarity. Reagents: (a) $Zn(OAc)_2$ and $La(OAc)_3$, (b) 1,2-bis(aminooxy)ethane and (c) dil. HCl.

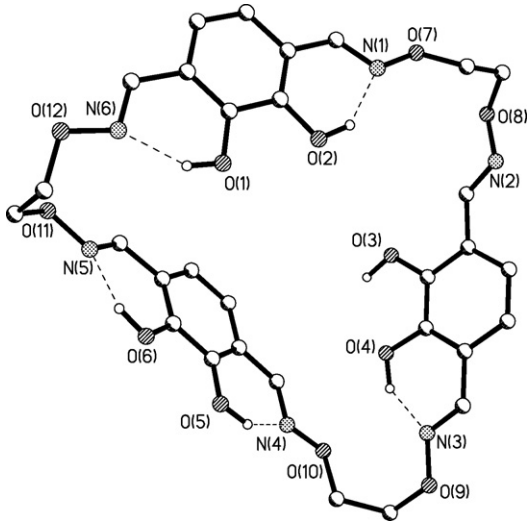

Fig. 20. Crystal structure of $H_6\mathbf{L^8}$. This picture was generated from the data available in the supporting information of Ref. [43]. Dotted lines indicate hydrogen-bonding interactions. Solvent molecules and hydrogen atoms not involved in hydrogen bonding have been omitted for clarity.

of **1** by coordination to the catechol oxygen donors and salicylaldehyde moieties, respectively. The metal ion template orients the three dialdehyde moieties appropriately for formation of the [3 + 3] macrocycle upon addition of the diamine. The template ions can be removed by treatment with dilute acid, with an excellent overall yield of 94%.

Unlike the Schiff base macrocycles $H_6\mathbf{L^6}$ and $H_6\mathbf{L^7}$, the non-templated preparation of $H_6\mathbf{L^8}$ produced the oxime macrocycle in only 15% yield (compared with 91% for $H_6\mathbf{L^6}$), even when carried out in high dilution. There are two potential reasons. First, the oxime bond is more resistant to metathesis (exchange) than the imine bond [43,49], and thus kinetically favoured products (i.e. other macrocycles and polymers) form with little subsequent bond exchange to alter the distribution of products. Second, the —O—CH_2CH_2—O— spacer of the amine is conformationally very flexible compared to the phenylene spacer of the amine used in the $H_6\mathbf{L^6}$ and $H_6\mathbf{L^7}$ macrocycles, tending to favour the formation of linear oligomers such as the [2 + 1] and [3 + 2] condensation products.

A single crystal structure determination on the macrocycle $H_6\mathbf{L^8}$ revealed that, as in $H_6\mathbf{L^6}$ and $H_6\mathbf{L^7}$, all of the catechol oxygen atoms are involved in hydrogen bonding to the nearest nitrogen atom (Fig. 20), except for O3 which hydrogen bonds to an ethanol solvent molecule. The catechol units are orientated away from the plane of the macrocycle to reduce repulsive interactions between the hydroxyl groups, again as with $H_6\mathbf{L^6}$ and $H_6\mathbf{L^7}$.

Attempting to synthesize a macrocycle containing different imine bonds, by stepwise addition of components, will often lead to a mixture of products because of bond exchange. However, MacLachlan and co-workers have successfully exploited the difference in stability of imines derived from aldehydes (aldimines) compared to those derived from ketones (ketimines) to prepare macrocycles with two chemically inequivalent imine bonds [19]. Using a small model system, in hot acetonitrile, aldimine bonds are labile whereas ketimine bonds are inert. Therefore, once a suitable ketimine is prepared, it can be involved in further imine formation without fear of exchange. In the first step the ketimine is prepared, from the diketone **5** and two equivalents of the diamine, and can be isolated if desired. One of the two amine moieties of each phenylenediamine remains unreacted because harsh conditions are required for reaction at both sites when a diphenyl ketone is involved [50]. The ketimine is then reacted with the dialdehyde **1**

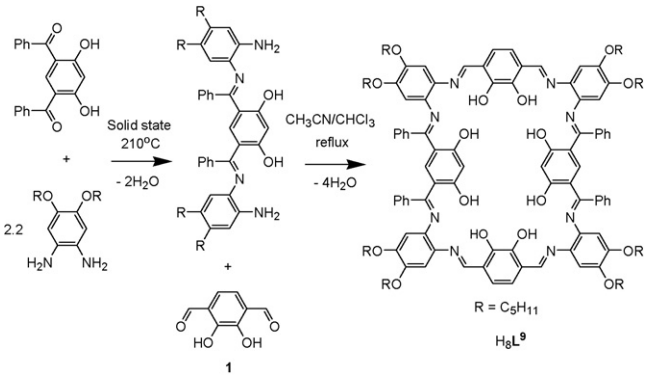

Fig. 21. Stepwise preparation of the macrocycle $H_8\mathbf{L^9}$.

in $CH_3CN/CHCl_3$, forming the macrocycle $H_8\mathbf{L^9}$ in 35% yield following recrystallization (Fig. 21). No side-products are generated from hydrolysis of the ketimine and the subsequent reaction between **1** and the phenylenediamine, which coincidentally would form $H_6\mathbf{L^7}$.

In the same manner as for $H_8\mathbf{L^9}$, the diketone **3** has been used by MacLachlan and co-workers to create a conjugated macrocycle with inequivalent imine bonds, $H_8\mathbf{L^{10}}$ (Fig. 22).

Like dialdehyde **1**, **2** has also been used to create [3 + 3] macrocycles. Reaction of **2** with the appropriate diamine in $CHCl_3$, followed by concentration of the reaction solution and the addition of MeCN, results in the precipitation of the macrocycle $H_6\mathbf{L^{11}}$ in 46% yield (Fig. 23) [17]. In a similar manner to $H_6\mathbf{L^6}$ and $H_6\mathbf{L^7}$, this metal free preparation of $H_6\mathbf{L^{11}}$ is facilitated by the reversibility of the imine bond formation, allowing the most thermodynamically stable product to form over polymers and oligomers. No metal ion complexes of $H_6\mathbf{L^{11}}$ have been published to date.

Interestingly, various data indicated that $H_6\mathbf{L^{11}}$ exists as a mixture of two tautomeric forms. The IR and UV–vis spectrum of $H_6\mathbf{L^{11}}$ is substantially different to that of $H_6\mathbf{L^7}$ (a macrocycle known to be in the enol form), suggesting a significant difference in structure. X-ray crystallography on model compounds, at −100 °C, showed that the 'enol' form is less prevalent than the 'keto-enamine' form (Fig. 24). Specifically because the C—O bonds lengths are closer to double rather than single bonds, and each nitrogen (not oxygen) atom is bonded to a hydrogen atom (located from the difference map). Ab initio DFT calculations also indicated that the keto-enamine form is around 0.7 kcal/mol more stable than the enol form. At room temperature in $CDCl_3$, the mixture of tautomers in the model compound was found by VT ^{13}C NMR and calculations

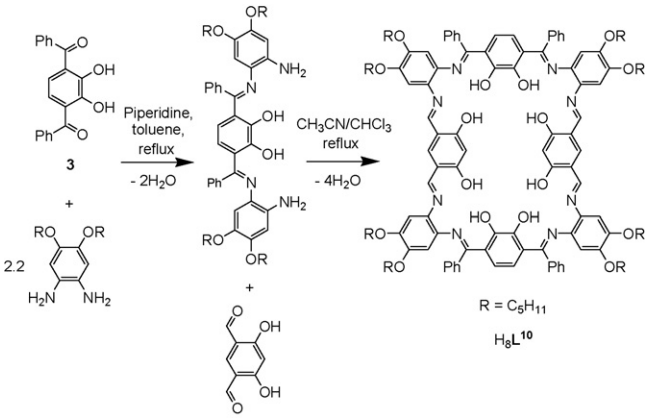

Fig. 22. Stepwise preparation of the macrocycle $H_8\mathbf{L^{10}}$.

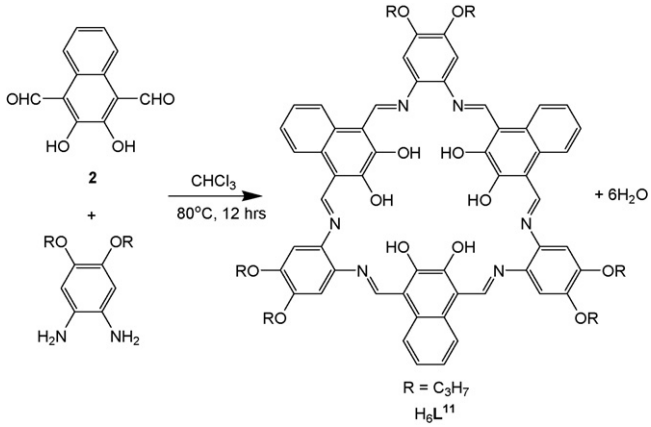

Fig. 23. Preparation of the macrocycle $H_6\mathbf{L^{11}}$.

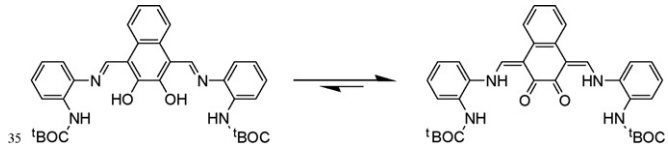

Fig. 24. Tautomerization observed for the model system of $H_6\mathbf{L^{11}}$. Enol form (LHS) and keto-enamine form (RHS).

to be 4:1 keto:enol. Formation of the more stable keto-enamine tautomer must be a sufficient driving force to overcome the accompanying loss of aromaticity in one of the two aromatic rings. At the time of writing the complexation chemistry of this macrocycle was under investigation [17].

Using **2**, Reinhoudt and co-workers synthesized three [3+3] macrocycles, $H_6\mathbf{L^{12}}$, $H_6\mathbf{L^{13}}$ and $H_6\mathbf{L^{14}}$ (Fig. 25), and one [4+4] macrocycle, $H_8\mathbf{L^{15}}$ (Fig. 26), as barium complexes [18]. The $[Ba(H_6\mathbf{L^n})](CF_3SO_3)_2$ n = 12–14 complexes are prepared by refluxing three equivalents of the dialdehyde **2** in MeCN/MeOH with one equivalent of $Ba(CF_3SO_2)_2$ before adding three equivalents of the appropriate diamine and refluxing for one hour. The macrocyclic complexes are precipitated, in approximately 70% yield, from the cooled solution by addition of diisopropyl ether.

The barium complex of the [4+4] macrocycle $H_4\mathbf{L^{15}}$ (Fig. 26) is synthesized in an analogous manner, but using a different diamine, 1,3-diaminpropane. The same molar ratio of Ba^{2+}:**2**:diamine is used (1:3:3) but the condensation generates [3+3] and some [4+4] product at reflux, but mainly [4+4] and some [2+2] product at room temperature. At room temperature the mixture, primarily $[Ba(H_6\mathbf{L^{15}})](CF_3SO_3)_2$, is obtained in 60% yield.

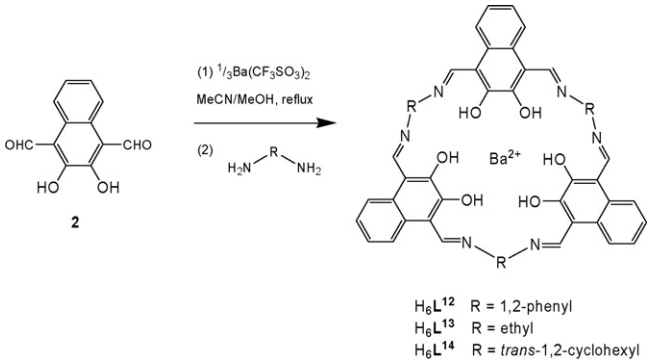

Fig. 25. Preparation of the macrocycles $H_8\mathbf{L^{12}}$, $H_8\mathbf{L^{13}}$ and $H_8\mathbf{L^{14}}$.

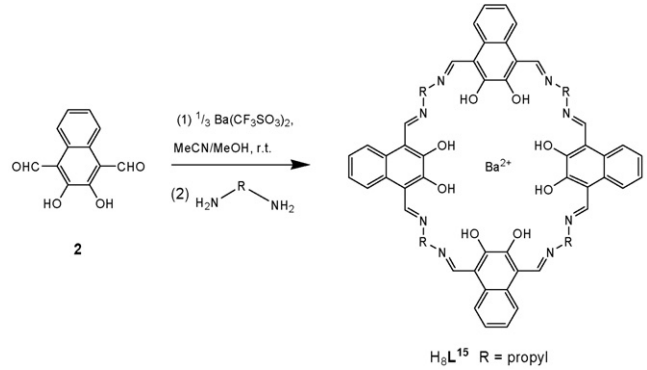

Fig. 26. Preparation of the macrocycle $H_8\mathbf{L^{15}}$.

3.2. Homometallic complexes

Both the Nabeshima and MacLachlan groups have investigated metal complexes of $H_6\mathbf{L^7}$ (Fig. 17). Nabeshima and co-workers treated $H_6\mathbf{L^7}$ (where R = C_4H_9) in $CHCl_3$ with an excess of $Zn(OAc)_2$ in MeOH to create the red *homoheptametallic* cluster $[Zn_7(\mathbf{L^7})O(OAc)_6]$ [47]. The yield of the complex varied depending on the chain length (91% for R = C_4H_9, 71% for R = C_8H_{17}). The heptametallic Zn^{2+} complex with R = $C_{12}H_{25}$ could be formed in 87% yield if the condensation between 3 equivalents of dialdehyde and 3 equivalents of diamine was carried out in the presence of seven equivalents of Zn^{2+}. *Homohexametallic* Zn_6 complexes of $H_6\mathbf{L^7}$ were also formed as side products of formation of the heptametallic cluster. MacLachlan and co-workers had also synthesized the $[Zn_7(\mathbf{L^7})O(OAc)_6]$ complex using different alkoxy chain lengths (R = C_2H_5, C_5H_{11}, C_6H_{13} and $CH_2{}^tBu$) to that used by the Nabeshima group.

The crystal structures of $[Zn_7(\mathbf{L^7})O(OAc)_6]$ have been reported by Nabeshima, where R = C_4H_9 [47], and by MacLachlan, where R = C_2H_5 [51], C_5H_{11} [51] and $CH_2{}^tBu$ [52]. Crystal structures have not been reported for the analogous complexes with R = C_8H_{17} and $C_{12}H_{25}$ but characterisation by ESI-MS, ^1H NMR spectroscopy, UV–vis spectroscopy and microanalysis indicates that they have analogous structures to those determined for the other chain lengths [46].

Other than the differing chain lengths, the structures of these $[Zn_7(\mathbf{L^7})O(OAc)_6]$ complexes are all remarkably similar. The complex where R = C_2H_5 contains a coordinated DMSO molecule from the recystallization solvent. The complex $[Zn_7(\mathbf{L^7})O(OAc)_6]$ where R = C_4H_9 is shown in Fig. 27 to illustrate the structural features of

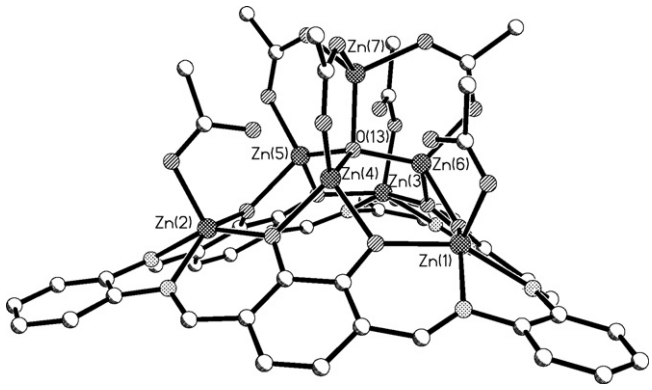

Fig. 27. Crystal structure of $[Zn_7(\mathbf{L^7})O(OAc)_6]$. This figure was generated from data obtained from the Cambridge Crystallographic Data Centre as published originally in Ref. [47]. The OC_4H_9 chains, disordered atoms, hydrogen atoms and solvent molecules have been submitted for clarity.

these $[Zn_7(\mathbf{L^7})O(OAc)_6]$ complexes. Three of the Zn^{2+} ions (Zn1, Zn2 and Zn3) occupy the three N_2O_2 pockets of the macrocycle. The macrocycle itself is non-planar—adopting a 'bowl-shaped' concave conformation. Sitting above the macrocycle is an oxide ion (O13) with four Zn^{2+} ions tetrahedrally arranged around it (Zn4, Zn5, Zn6 and Zn7). This 'core' is bound to the macrocycle by the three Zn^{2+} ions at the base of tetrahedron (Zn4, Zn5 and Zn6), each of which are bound to two catechol oxygens of the macrocycle [47]. Zn1, Zn2 and Zn3 each have coordinated acetate bound through only one of the oxygen donor atoms, while Zn4, Zn5 and Zn6 are all bridged to Zn7 by an acetate ligand.

The 'core' described above consists of $[Zn_4O(OAc)_6]$ and can be roughly approximated as a subunit of the complex that is bound to the distorted macrocycle through the catechol oxygen donor atoms. The resemblance of this subunit to basic zinc acetate prompted MacLachlan and co-workers to investigate the mechanism of formation of the heptametallic zinc complex [52]. Either, basic zinc acetate is formed in solution and coordinates to the trimetallated macrocycle, or the macrocycle templates the formation of the complex in a stepwise fashion. The stepwise formation of the complex was hypothesized to be more likely, as the heptametallic complex can be made at room temperature and ambient pressure, while the creation of basic zinc acetate requires heat and a vacuum.

To obtain evidence for the stepwise formation of $[Zn_7(\mathbf{L^7})O(OAc)_6]$ MacLachlan and co-workers synthesized a *tetrametallic* intermediate. The macrocycle $H_6\mathbf{L^7}$ (where $R = CH_2{}^tBu$) was reacted with four equivalents of $Zn(OAc)_2$ in EtOH and the resulting complex characterised by ^1H NMR, MALDI-TOF mass spectrometry and X-ray crystallography. The product was the tetrametallic complex $[Zn_4(\mathbf{L^7})(H_2O)(OAc)_2]$ in which all three N_2O_2 pockets of the macrocycle were occupied by zinc ions, while the fourth zinc ion was bound to two catecholate oxygen donors (in the position it would have been in the complete heptametallic complex). A water molecule coordinated to the fourth zinc ion was positioned appropriately to become the central oxide ion of $[Zn_7(\mathbf{L^7})O(OAc)_6]$. To obtain further evidence for the stepwise mechanism the macrocycle $H_6\mathbf{L^7}$ with $R = CH_2{}^tBu$ was reacted with four equivalents of zinc methacrylate [52]. From this reaction a *tetrametallic* complex similar to $[Zn_4(\mathbf{L^7})H_2O(OAc)_2]$ was obtained, with methacrylate ligands in place of the acetate ligands. Again, a water ligand was directed towards the centre of the macrocycle, in a similar position to the central oxide ion of the heptametallic zinc cluster. A ^1H NMR titration experiment on $[Zn_4(\mathbf{L^7})(H_2O)(OAc)_2]$ indicated the potential existence of other intermediates, although none could be isolated. The authors hypothesize that the rigid nature of the macrocycle prevents the Zn^{2+} ions in the N_2O_2 pockets from obtaining a tetrahedral geometry, and that as a result they adopt a pseudo-square planar geometry. This permits a carboxylate ligand to bind in the apical position (resulting in the distorted square pyramidal geometry seen in $[Zn_7(\mathbf{L^7})O(OAc)_6]$) and creates a scaffold for templation of the remaining $Zn_4O(OAc)_6$ core.

In a recent publication [46], Nabeshima and co-workers reported that the reaction of Co^{2+}, Ni^{2+}, Mn^{2+} or Cu^{2+} acetate with $H_6\mathbf{L^7}$ (where $R = C_4H_9$) gave a number of different homometallic complexes. Unfortunately, crystal structures were not reported for any of these complexes. Instead, sporting methods (ESI-MS, UV–vis spectroscopy and elemental analysis) were used to tentatively identify the nuclearity and oxidation states of the complexes. Colours and yields were not detailed for all of the complexes but those that were specified are provided here.

A number of different polymetallic manganese complexes could be readily prepared by the reaction of $H_6\mathbf{L^7}$ with $R = C_4H_9$ in CH_2Cl_2 with $Mn(OAc)_2{\cdot}4H_2O$ in MeOH [46]. Addition of three equivalents of Mn^{2+} to a solution of $H_6\mathbf{L^7}$ resulted in the formation of the *trimetallic* complex Mn^{2+} complex, that oxidized to $[Mn^{III}{}_3(\mathbf{L^7})]^{3+}$ when deliberately exposed to air. When repeated under an inert atmosphere, the Mn^{2+} ions remained in the 2^+ state until, again, oxygen was deliberately introduced, converting the UV–vis spectrum to one which was identical to $[Mn_3{}^{III}(\mathbf{L^7})]^{3+}$. Complexation of three equivalents of $Mn(OAc)_2$ with $H_6\mathbf{L^7}$ in air resulted in smooth oxidation of the Mn^{2+} ions to the 3^+ state. When $H_6\mathbf{L^7}$ with $R = C_4H_9$ was reacted with 10 equivalents of Mn^{2+}, black crystals of the resulting *heptametallic* complex $[Mn^{II}{}_7(\mathbf{L^7})(O)(OAc)_6]{\cdot}4H_2O$ were isolated in excellent, 97%, yield. This complex and its *hexametallic* analogue (not isolated) were reported to be significantly more stable to oxidation than the trimetallic complex. However, partially oxidized species such as $[Mn^{III}Mn^{II}{}_6(\mathbf{L^7})(O)(OAc)_5]^{2+}$ were detected in the mass spectrum.

Tri- and *hexametallic* Ni^{2+} complexes were formed by the reaction of $H_6\mathbf{L^7}$ with $R = C_4H_9$ in $CHCl_3$ with $Ni(OAc)_2{\cdot}4H_2O$ in MeOH [46]. Addition of three equivalents of Ni^{2+} to a solution of $H_6\mathbf{L^7}$ formed the trimetallic complex $[Ni_3(\mathbf{L^7})]{\cdot}CHCl_3{\cdot}H_2O$ in 78% yield. The use of 10 equivalents, however, resulted in formation of the *hexametallic* analogue. Unlike with Zn^{2+} and Mn^{2+}, no heptametallic Ni^{2+} complexes could be prepared, even in the presence of excess (10 equivalents) Ni^{2+}. When bound to a Ni^{2+} ion, a planar salen ligand with a phenylene spacer shows a strong absorbance at λ_{max} of 480 nm. This absorbance was not seen in $[Ni_3(\mathbf{L^7})]{\cdot}CHCl_3{\cdot}H_2O$, indicating that the three salen-style subunits of the *trimetallic* complex are non-planar.

In contrast to the other metal ions investigated, only *trimetallic* complexes could be obtained when $H_6\mathbf{L^7}$ with $R = C_4H_9$ in $CHCl_3$ was reacted with Co^{2+} or Cu^{2+} acetate in MeOH, even with an excess of metal [46]. Addition of three equivalents of $Co(OAc)_2{\cdot}4H_2O$ to a solution of $H_6\mathbf{L^7}$ resulted in the formation of $[Co^{II}{}_3(\mathbf{L^7})(OAc)_3]{\cdot}2H_2O$, a black powder, in 70% yield. The Co^{2+} ions in this complex can also be oxidized by air to Co^{3+}, but at a much slower rate than with Mn^{2+}, as indicated by the rate at which the UV–vis spectrum of $[Co^{II}{}_3(\mathbf{L^7})]{\cdot}2H_2O$ changed to that observed for $[Co^{III}{}_3(\mathbf{L^7})]^{3+}$. A *trimetallic* Cu^{2+} complex $[Cu_3(\mathbf{L^7})]{\cdot}CHCl_3{\cdot}H_2O$, was also prepared, in 80% yield, by the addition of three equivalents of $Cu(OAc)_2{\cdot}H_2O$ to a solution of $H_6\mathbf{L^7}$. Higher nuclearity complexes of Co^{3+} and Cu^{2+} could not be prepared even in the presence of excess (10 equivalents) of the metal salts.

Recently, MacLachlan and co-workers have created two *heptametallic* cadmium complexes of the macrocycle $H_6\mathbf{L^7}$; $[Cd_7(\mathbf{L^7})O(OAc)_6(H_2O)_3]$ where $R = C_2H_5$ and C_8H_{17} [53]. The complexes are synthesized by reacting $H_6\mathbf{L^7}$ with seven equivalents of $Cd(OAc)_2$ in EtOH, in a manner similar to the above heptazinc complex [54]. Although both the zinc and cadmium complexes contain seven metal ions they are not structurally equivalent. In fact, the differences in the coordination behaviour of Cd^{2+} versus Zn^{2+} results in the macrocycle being distorted into a more concave geometry than in $[Zn_7(\mathbf{L^7})O(OAc)_6]$. The X-ray crystal structure determination also revealed that the molecules of $[Cd_7(\mathbf{L^7})O(OAc)_6(H_2O)_3]$ with $R = C_2H_5$ dimerize in a 'face-to-face' fashion, stabilized by a number of weak CH. . .π interactions. Consequently, a capsule is formed in the space between the complexes. The room temperature ^1H NMR spectrum of $[Cd_7(\mathbf{L^7})O(OAc)_6(H_2O)_3]$ (where $R = OC_2H_5$) in DMF-d_7 showed broadening of the peaks associated with the complex, consistent with the dimerization noted in the solid state. Cooling the solution resulted in further broadening of the peaks until eventually they split into two sets of resonances, one for the monomer and one for the dimer. By recording the ^1H NMR spectrum of the complex at 238, 247, 256 and 265 K, and measuring the integration of the aromatic protons, the association constants of the dimer at different temperatures were obtained. The resulting van't Hoff plot suggested, surprisingly, that association was an *entropy*-driven process. Although self-association usually imparts order [53], the dimerization of the cadmium complex results in expulsion of a DMF

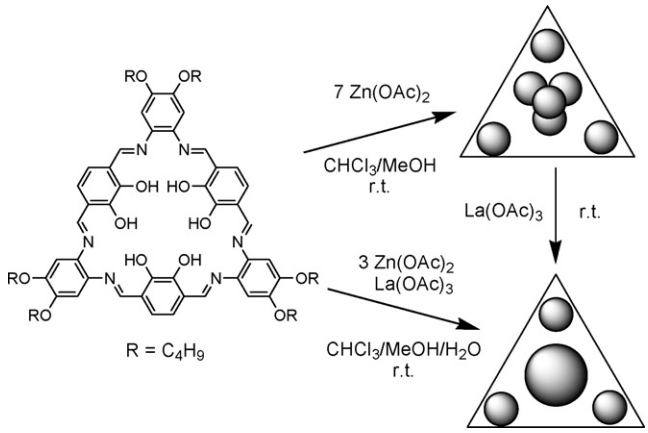

Fig. 28. Schematic representation of the complexation and transmetallation of $H_6\mathbf{L^7}$. Small sphere = Zn; large sphere = La.

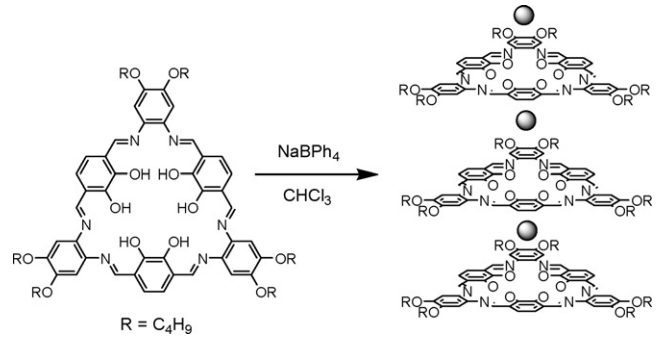

Fig. 29. Postulated structure of metal ion-induced assembly of tubes of $H_6\mathbf{L^7}$ using Na^+ (depicted as a sphere on the RHS). The distance between macrocycles has been exaggerated for clarity.

molecule from the capsule and an increase in entropy in the system of $110 \pm 2\,J\,mol^{-1}\,K^{-1}$. Dimerization of $[Zn_7(\mathbf{L^7})O(OAc)_6]$ with $R = C_8H_{17}$ is also an entropy-driven process, however the association constant is $10 \pm 3\,L\,mol^{-1}$ compared with $270 \pm 10\,L\,mol^{-1}$ for the cadmium complex. The cadmium complex with $R = C_8H_{17}$ was soluble in aromatic solvents (benzene-d_7, toluene-d_8 and xylene-d_{10}) and again the room temperature ^1H NMR spectra showed significant broadening of peaks. ^1H NMR spectra at various temperatures were therefore recorded to probe the strength of dimerization. Unlike $[Cd_7(\mathbf{L^7})O(OAc)_6(H_2O)_3]$ where $R = C_2H_5$, no distinct sets of signals corresponding to monomer or dimer forms could be identified. However, the change in chemical shift of the imine proton as a function of concentration allowed a van't Hoff plot to be constructed and association constants to be obtained and compared to the DMF-soluble complex. The constants for the aromatics-soluble complex were larger (800, 1000 and $1500\,L\,mol^{-1}$ for benzene-d_7, xylene-d_{10} and toluene-d_8, respectively) than the DMF-soluble analogue but were of the same general magnitude.

Fast atom bombardment (FAB) mass spectrometry indicates that the macrocycles $H_6\mathbf{L^{12\text{-}14}}$ and $H_8\mathbf{L^{15}}$ form tetranuclear complexes with transition metal ions such as Cu^{II}, Ni^{II} and Zn^{II} [18]. No structures were reported for these complexes.

3.3. Heterometallic complexes

Nabeshima and co-workers have experimented with transmetallation of the homometallic Zn_7 complex $[Zn_7(\mathbf{L^7})O(OAc)_6]$ with $R = C_4H_9$. It can be converted to a dark red *heterotetrametallic* analogue $[Zn_3La(\mathbf{L^7})]$, by treatment with one equivalent of $La(OAc)_3$ (Fig. 28) [47].

The La^{3+} ion appears to displace the four Zn^{2+} ions of the tetrahedral core and the macrocycle is expected to return to a planar conformation, although this is yet to be confirmed by crystal structure determination. This heterometallic complex can also be prepared in 91% yield by a one-pot reaction of one equivalent of $H_6\mathbf{L^7}$, three equivalents of $Zn(OAc)_2$ and one equivalent of $La(OAc)_3$. In the ESI mass spectrum of this heterometallic Zn_3La complex, peaks at high m/z suggest that the complex also aggregates into a dimer, trimer and tetramer. No mechanism for this aggregation is tendered, though it is thought to be facilitated by the more planar structure of $[Zn_3La(\mathbf{L^7})]$ than $[Zn_7(\mathbf{L^7})O(OAc)_6]$.

MacLachlan and co-workers have also investigated the formation of mixed-metal complexes of $H_6\mathbf{L^7}$ with $R = CH_2{}^tBu$. Reaction of the *homotetrametallic* complex $[Zn_4(\mathbf{L^7})H_2O(OAc)_2]$ with four equivalents of $Co(OAc)_2$ in refluxing EtOH resulted in the formation of a mixture of heterometallic complexes, as determined by MALDI-TOF mass spectrometry. Peaks were observed for $[Zn_4Co_3(\mathbf{L^7})O(OAc)_5]^+$, $[Zn_3Co_4(\mathbf{L^7})(OAc)_5]^+$ and $[Zn_3Co_3(\mathbf{L^7})(OAc)_3]^+$ [54]. The *heterohexametallic* complex was suspected to be a fragmentation of a *heteroheptametallic* complex.

The MacLachlan group has also experimented with the self-assembly of $H_6\mathbf{L^7}$ into supramolecular architectures in solution upon coordination to metal ions [2]. Molecules of $H_6\mathbf{L^7}$ with $R = C_6H_{13}$ were shown to organize into tubular structures with each macrocycle linked to another above and below it by small monovalent metal cations such as Na^+ (Fig. 29), K^+ and Cs^+. The aggregation was deduced from analysis of ESI-MS data, UV–vis and ^1H NMR spectra. In the assemblies, the small cations were thought to be coordinated to the central phenolic oxygen atoms, rather than in the N_2O_2 pockets. The tubular assemblies were only observed at high metal:ligand ratios; at lower metal ion concentrations, metal ion-bridged dimers and trimers are predominately obtained. Furthermore, macrocycles were found to be transferring between aggregates.

Although the coordination chemistry of the macrocycle $H_6\mathbf{L^8}$ (Fig. 19) is not discussed in detail, preliminary investigations suggest that it forms homometallic complexes such as $[Zn_6(\mathbf{L^8})(OAc)_5(OH)(MeOH)]$ that contain six transition metal ions, and heterometallic complexes such as $[Zn_3La(\mathbf{L^8})(NO_3)_3(MeOH)_2]$ containing three transition metal ions and one lanthanide ion [43]. The coordination chemistry of the macrocycle $H_8\mathbf{L^9}$ was being further investigated at the time of writing [43].

4. Concluding remarks

In summary, a significant number of intriguing acyclic and macrocyclic ligands and polymetallic complexes derived from **1** have been reported, to date exclusively by the groups of Nabeshima and MacLachlan. One acyclic and six macrocyclic ligand structures have been reported (Table 1). Of the 41 complexes that have been structurally characterised (Tables 2 and 3), to date, all of the complexes of the acyclic ligands have one of just three types of structural motifs **A**–**C** (Fig. 30) and all of the complexes of the macrocyclic ligands have one of just four types of structural motifs **D**–**G** (Fig. 30). In both cases these motifs may be further elaborated on by a number of other ligands such as acetate ions, nitrate ions, water and alcohol solvent molecules.

This head unit, **1**, provides a valuable platform for generating polymetallic complexes featuring bridging of the metal ions. In addition, it provides access to [3 + 3] macrocycles and hence trimetallic/triangular macrocyclic complexes, both of which are relatively unusual. In this review we have tried to highlight the breadth and richness of the chemistry generated from **1** to date, and to sig-

Table 1
Schematic diagrams and perspective views of the structurally characterised ligands derived from **1** that either appear in the CSD (Version 5.29, released November, 2007) [55] or have been published since. For clarity, non-coordinated solvent molecules and hydrogen atoms have been excluded.

Formula of structure	Schematic	Crystal structure	CSD ref. code	Ref.
H_4L^1	Fig. 8	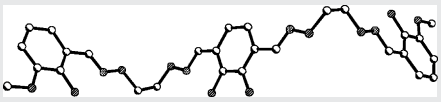	–	[35]
$H_6L^6 \cdot 3MeCN$	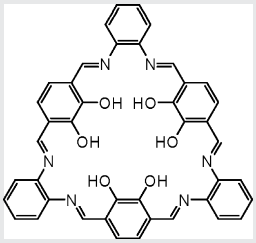	Similar to CACYEL	CACYAH	[1]
$H_6L^6 \cdot H_2O \cdot MeCN$	Similar to CACYAH	Fig. 16	CACYEL	[1]
$H_6L^7 \cdot 6DMF$ (R = C_2H_5)	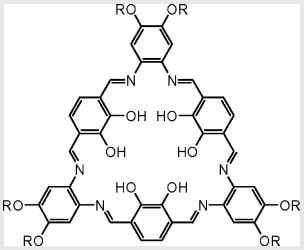	Similar to CACYEL	DAWREZ	[45]
$H_6L^7 \cdot H_2O$ (R = C_6H_{13})	Similar to DAWREZ	Similar to CACYEL	FANTEU	[48]
$H_6L^8 \cdot EtOH$	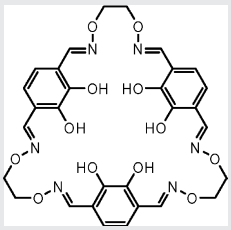	Fig. 20	HICLEL	[43]
$H_6L^7 \cdot 2CH_2Cl_2$ (R = C_4H_9)	Similar to DAWREZ	Similar to CACYEL	NENHIY	[47]

Table 2
Structural motifs and perspective views of the structurally characterised complexes of acyclic ligands derived from **1** that either appear in the CSD (Version 5.29, released November, 2007) [55] or have been published since. For clarity, non-coordinated solvent molecules and hydrogen atoms have been excluded.

Formula of structure	Structural motif (Fig. 30)	Crystal structure	CSD ref. code	Ref.
$[Zn_3(L^1)(OAc)_2(H_2O)] \cdot C_3H_6O$	A	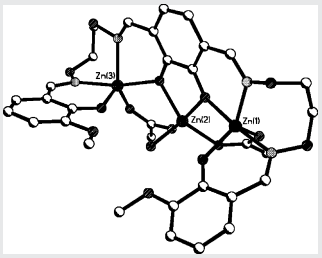	PEWGEE	[14]
$[Zn_3(L^2)(OAc)_2(H_2O)] \cdot 2C_3H_6O$	A	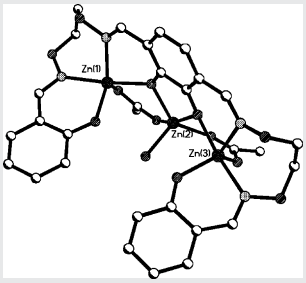	PEWGII	[14]

Table 2 (*Continued*)

Formula of structure	Structural motif (Fig. 30)	Crystal structure	CSD ref. code	Ref.
$[Zn_3(L^1)(OAc)_2(EtOH)]\cdot 0.5CHCl_3\cdot 0.5C_3H_6O$	A	Fig. 9	WURBEQ	[24]
$[Zn_3(L^4)(OAc)_2(MeOH)_2]\cdot CHCl_3$	A	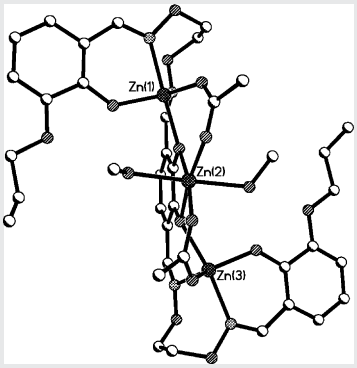	CIVBIT	[34]
$[Mn^{II}_3(L^1)(OAc)_2(MeOH)_2]$	A	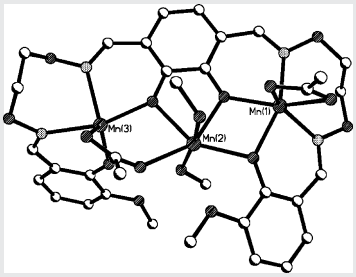	–	[35]
$[Co^{II}_3(L^1)(OAc)_2(EtOH)_2]\cdot 2CHCl_3$	A	Fig. 9	–	[35]
$[Zn_2Mn^{II}(L^1)(OAc)_2(MeOH)_2]$	A	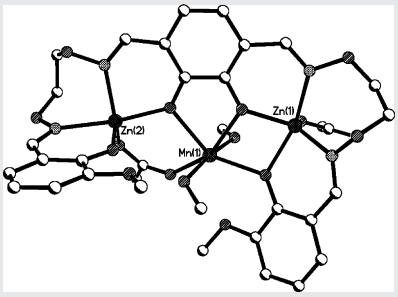	–	[35]
$[Cu_2Zn(L^1)(OAc)_2(H_2O)]\cdot MeOH\cdot 8.5H_2O$	A	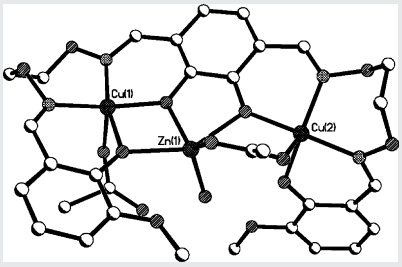	–	[35]
$[Zn_2Ca(L^1)(MeOH)_2(ClO_4)_2]$	B	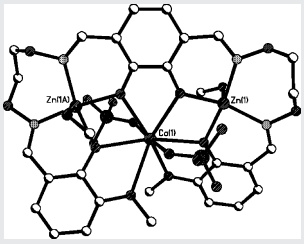	FELBUU, FELBUU01	[14,23]

Table 2 (*Continued*)

Formula of structure	Structural motif (Fig. 30)	Crystal structure	CSD ref. code	Ref.
$[Cu_2Gd(L^1)(OAc)_3]\cdot Et_2O\cdot EtOH$	B	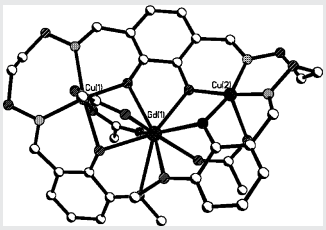	GANFAD	[36]
$[Zn_2Ce(L^1)(OAc)_3]\cdot 3MeOH\cdot CHCl_3$	B	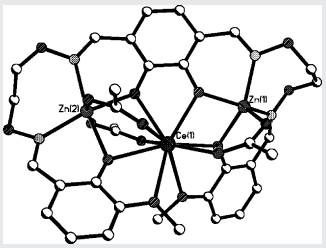	PEWBUP	[14]
$[Zn_2Pr(L^1)(OAc)_3]\cdot 3MeOH\cdot CHCl_3\cdot 0.25H_2O$	B	Similar to PEWBUP	PEWCAW	[14]
$[Zn_2Nd(L^1)(OAc)_3]\cdot 3MeOH\cdot CHCl_3\cdot 0.25H_2O$	B	Similar to PEWBUP	PEWCEA	[14]
$[Zn_2Eu(L^1)(OAc)_3]\cdot 3MeOH\cdot CHCl_3$	B	Similar to PEWBUP	PEWCIE	[14]
$[Zn_2Sm(L^1)(OAc)_3]\cdot 3MeOH\cdot CHCl_3$	B	Similar to PEWBUP	PEWCOK	[14]
$[Zn_2Gd(L^1)(OAc)_3]\cdot 2.8MeOH\cdot CHCl_3\cdot 05H_2O$	B	Similar to PEWBUP	PEWCUQ	[14]
$[Zn_2Tb(L^1)(OAc)_3(MeOH)]\cdot Et_2O\cdot H_2O$	B	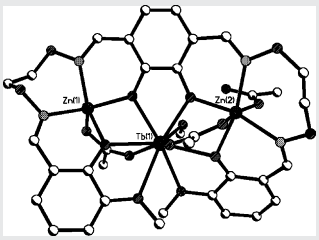	PEWDAX	[14]
$[Zn_2Dy(L^1)(OAc)_3(MeOH)]\cdot Et_2O\cdot H_2O$	B	Similar to PEWDAX	PEWDEB	[14]
$[Zn_2Ho(L^1)(OAc)_3(MeOH)]\cdot Et_2O\cdot H_2O$	B	Similar to PEWDAX	PEWDIF	[14]
$[Zn_2Er(L^1)(OAc)_3(MeOH)]\cdot Et_2O\cdot H_2O$	B	Similar to PEWDAX	PEWDOL	[14]
$[Zn_2Tm(L^1)(OAc)_3(H_2O)]\cdot CHCl_3$	B	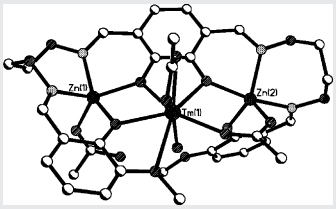	PEWDUR	[14]
$[Zn_2Yb(L^1)(OAc)_3(H_2O)]\cdot CHCl_3$	B	Similar to PEWDUR	PEWFAZ	[14]
$[Zn_2Lu(L^1)(OAc)_3(H_2O)]\cdot C_3H_6O$	B	Similar to PEWDUR	PEWFED	[14]
$[Zn_2Sc(L^1)(OAc)_2(MeOH)_2](NO_3)\cdot EtOH\cdot MeOH$	B	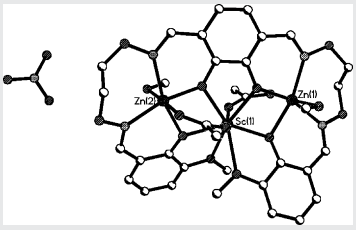	PEWFIN	[14]
$[Zn_2Y(L^1)(OAc)_2(MeOH)(NO_3)]\cdot MeOH$	B	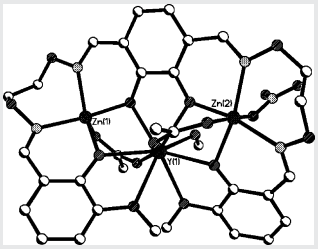	PEWFON	[14]

Table 2 (*Continued*)

Formula of structure	Structural motif (Fig. 30)	Crystal structure	CSD ref. code	Ref.
$[Zn_2Sr(L^1)(OAc)_2]\cdot CH_2Cl_2$	B	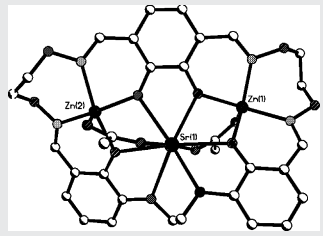	PEWFUT	[14]
$[Zn_2Ba(L^1)(OAc)_2]\cdot 0.5CHCl_3\cdot Et_2O\cdot 1.5H_2O$	B	Similar to PEWFUT	PEWGAA	[14]
$[Zn_2La(L^1)(OAc)_3]\cdot 2CHCl_3$	B	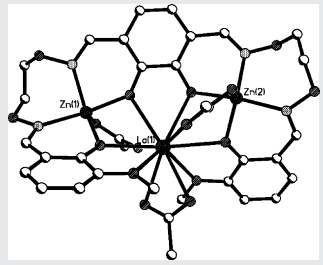	PEWGOO	[14]
$[Zn_2Eu(L^1)(OAc)_2(NO_3)(H_2O)]\cdot 3.5C_3H_6O$	B	Fig. 11	WURBIU	[24]
$[Zn_2Ca(L^4)(OAc)_2]\cdot 0.5CHCl_3\cdot 0.75H_2O$	B	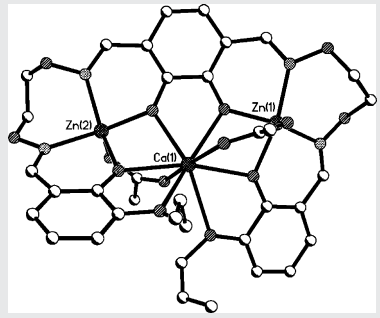	CIVBAL	[34]
$[Zn_2La(L^4)(OAc)_3]\cdot CHCl_3$	B	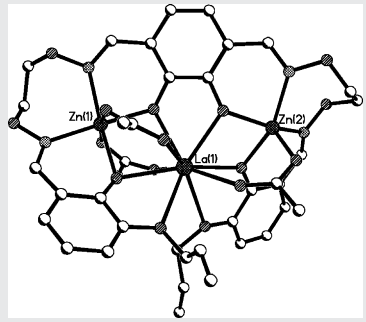	CIVBEP	[34]
$Zn_3La(L^5)(OAc)_3(EtOH)]\cdot H_2O$	C	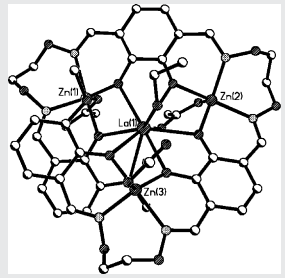	WESVAS	[32]

Table 3
Structural motifs and perspective views of the structurally characterised complexes of macrocyclic ligands derived from **1** that either appear in the CSD (Version 5.29, released November, 2007) [55] or have been published since. For clarity, non-coordinated solvent molecules, peripheral alkoxy chains of macrocycles and hydrogen atoms have been excluded.

Formula of structure	Structural motif (Fig. 30)	Crystal structure	CSD ref. code	Ref.
$[Zn_7(L^7)O(OAc)_6(DMSO)]\cdot 5DMSO$ ($R = C_2H_5$)	D	Similar to NENHOE	NELVOQ	[51]
$[Zn_7(L^7)O(OAc)_6]\cdot 2EtOAc\cdot THF$ ($R = C_4H_9$)	D	Fig. 27	NENHOE	[47]
$[Zn_7(L^7)O(OAc)_6]\cdot C_6H_6$ ($R = C_5H_{11}$)	D	Similar to NENHOE	NELVIK	[51]
$[Zn_7(L^7)O(OAc)_6]\cdot 7.5DMF$ ($R = CH_2{}^tBu$)	D	Similar to NENHOE	SIYPOG	[52]
$[Cd_7(L^7)O(OAc)_6(H_2O)_3]\cdot 7DMF$ ($R = C_2H_5$)	D	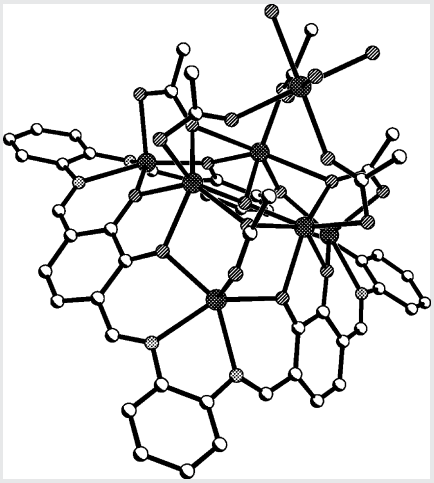	RIPZUM	[53]
$[Zn_4(L^7)(OAc)_2(H_2O)_2]\cdot 2.5DMF$ ($R = CH_2{}^tBu$)	E	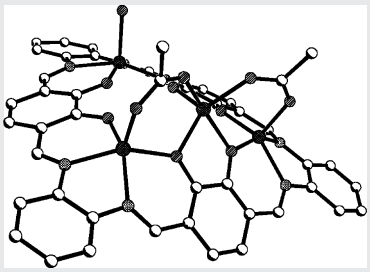	SIYPUM	[52]
$[Zn_4(L^7)(CH_3C(=CH_2)CO_2)_2(H_2O)(DMSO)]\cdot xDMSO$ ($R = CH_2{}^tBu$)	E	Similar to $[Zn_4(L^7)(OAc)_2(H_2O)_2]$	SIYQAT	[52]
$[Zn_6(L^8)(OAc)_5(OH)(MeOH]\cdot 2MeOH\cdot 1.5H_2O$	F	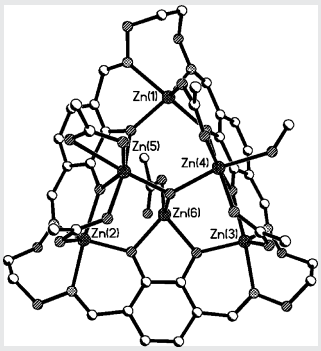	HICLUB	[43]
$[Zn_3La(L^8)(MeOH)_2(NO)_3]$	G	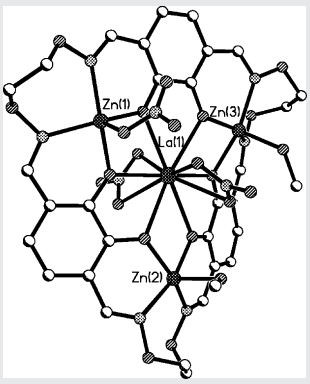	HICLOV	[43]

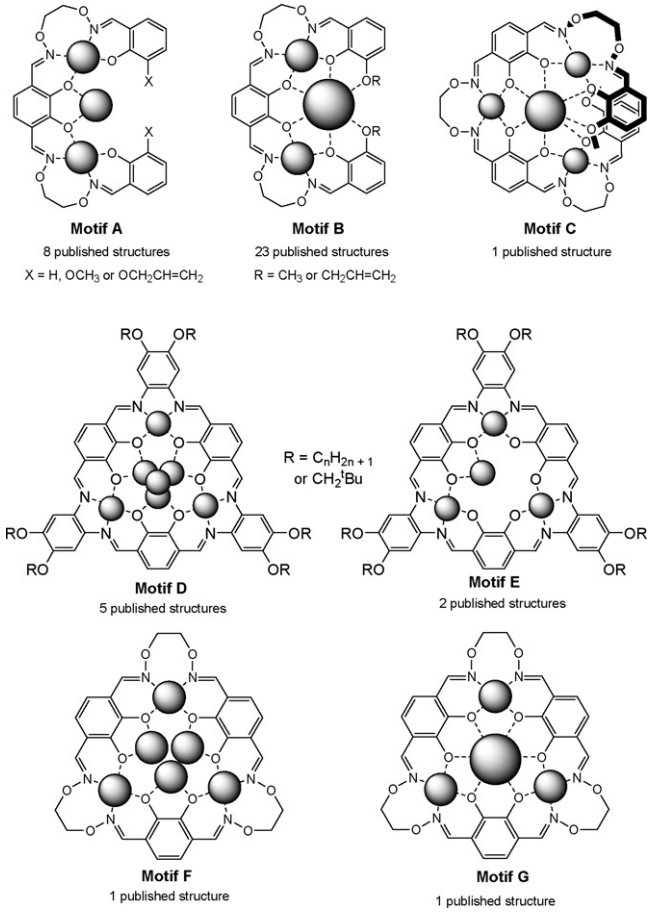

Fig. 30. To date, these are the only metal ion coordination motifs observed by X-ray crystallography for ligands derived from **1** (all other ligands are excluded from consideration here): acyclic (motifs **A**–**C**); macrocyclic (motifs **D**–**G**).

nal that there is a bright future ahead as this head unit, and its close analogues, continue to be put to new, exciting purposes.

Acknowledgements

This work was supported by grants from the University of Otago and the MacDiarmid Institute.

References

[1] S. Akine, T. Taniguchi, T. Nabeshima, Tetrahedron Lett. 42 (2001) 8861.
[2] A.J. Gallant, M.J. MacLachlan, Angew. Chem. Int. Ed. 42 (2003) 5307.
[3] H.G. McGuckin, J.S. Badger, B.M. Boersen, R. R. Horn, U.S., US 6,022,674, to Eastman Kodak Co., USA (2000).
[4] K. Akira, Jpn. Kokai Tokkyo Koho, JP 11065060, to Konica Co., Japan (1999).
[5] K. Takemura, Eur. Pat. Appl., Vol. EP 679940, Konica Co., Japan (1999).
[6] M. Hagiwara, S. Kuze, Jpn. Kokai Tokkyo Koho, JP 05045835, to Konishiroku Photo Ind., Japan (1993).
[7] M. Hagiwara, S. Kuze, Jpn. Kokai Tokkyo Koho, JP 05066538, to Konishiroku Photo Ind., Japan (1993).
[8] H. Kobayashi, S. Kuze, Jpn. Kokai Tokkyo Koho, JP 05088329, to Konishiroku Photo Ind., Japan (1993).
[9] K. Kuwae, S. Kuze, Jpn. Kokai Tokkyo Koho, JP 05080477, to Konishiroku Photo Ind., Japan (1993).
[10] H. Kobayashi, S. Kuse, Eur. Pat. Appl., EP 529794, to Konica Co., Japan (1993).
[11] K. Koma, S. Kuse, Eur. Pat. Appl., EP 530832 to Konica Co., Japan (1993).
[12] G.I. Georg, S.A. David, K. Khownium, S.J. Wood, K.A. Miller, R. Balakrishna, T.B. Nguyen, M.R. Kimbrell, Bioorg. Med. Chem. Lett. 16 (2006) 1305.
[13] M. Sauer, C. Yeung, J.H. Chong, B.O. Patrick, M.J. MacLachlan, J. Org. Chem. 71 (2006) 775.
[14] S. Akine, T. Taniguchi, T. Nabeshima, J. Am. Chem. Soc. 128 (2006) 15765.
[15] N. Kuhnert, G.M. Rossignolo, A. Lopez-Periago, Org. Biomol. Chem. 1 (2003) 1157.
[16] S. Patai, The Chemistry of the Carbon-Nitrogen Double Bond, John Wiley and Sons, 1970.
[17] A.J. Gallant, M. Yun, M. Sauer, C.S. Yeung, M.J. MacLachlan, Org. Lett. 7 (2005) 4827.
[18] W.T.S. Huck, F.C.J.M.v. Veggel, D.N. Reinhoudt, Recl. Trav. Chim. Pays-Bas. 114 (1995) 273.
[19] P.D. Frischmann, J. Jiang, J.K.H. Hui, J.J. Grzybowski, M.J. MacLachlan, Org. Lett. 10 (2008) 1255.
[20] S. Akine, T. Taniguchi, T. Nabeshima, Chem. Lett. (2001) 682.
[21] I.P. Singh, V.K. Shukla, A.K. Dwivedi, N.M. Khanna, Ind. J. Chem. 28b (1989) 692.
[22] A.H. Tran, D.O. Miller, P.E. Georghiou, J. Org. Chem. 70 (2005) 115.
[23] S. Akine, T. Taniguchi, T. Saiki, T. Nabeshima, J. Am. Chem. Soc. 127 (2005) 540.
[24] S. Akine, T. Takanori, T. Nabeshima, Angew. Chem. Int. Ed. 41 (2002) 4670.
[25] J.K.-H. Hui, M.J. MacLachlan, Chem. Commun. (2006) 2480.
[26] S. Akine, D. Hashimoto, T. Saiki, T. Nabeshima, Tetrahedron Lett. 45 (2004) 4225.
[27] B.N. Boden, A. Abdolmaleki, C.T.-Z. Ma, M.J. MacLachlan, Can. J. Chem. 86 (2008) 50.
[28] J. Sanmartin, M.R. Bermejo, A.M. Garcia-Deibe, O.R. Nascimento, A. Costa-Filho, Inorg. Chim. Acta 318 (2001) 135.
[29] J. Sanmartin, M.R. Bermejo, A.M. Garcia-Deibe, I.M. Rivas, A.R. Fernandez, J. Chem. Soc., Dalton Trans. (2000) 4174.
[30] S. Akine, W. Dong, T. Nabeshima, Inorg. Chem. 45 (2006) 4677.
[31] L. Salmon, P. Thuery, M. Ephritikhine, Polyhedron 23 (2004) 623.
[32] S. Akine, T. Taniguchi, T. Matsumoto, T. Nabeshima, Chem. Commun. 47 (2006) 4961.
[33] S. Akine, T. Taniguchi, T. Nabeshima, Tetrahedron Lett. 47 (2006) 8419.
[34] S. Akine, S. Kagiyama, T. Nabeshima, Inorg. Chem. 46 (2007) 9525.
[35] S. Akine, T. Taniguchi, T. Nabeshima, Inorg. Chem. 47 (2008) 3255.
[36] S. Akine, T. Matsumoto, T. Taniguchi, T. Nabeshima, Inorg. Chem. 44 (2005) 3270.
[37] V. Balzani, A. Credi, F.M. Raymo, J.F. Stoddart, Angew. Chem. Int. Ed. 39 (2000) 3348.
[38] D.E. Fenton, S.J. Kitchen, C.M. Spencer, S. Tamburini, P.A. Vigato, J. Chem. Soc., Dalton Trans. (1988) 685.
[39] B.F. Hoskins, R. Robson, P. Smith, J. Chem. Soc., Chem. Commun. (1990) 488.
[40] S.S. Tandon, L.K. Thompson, J.N. Bridson, J. Chem. Soc., Chem. Commun. (1992) 911.
[41] H.C. Aspinall, J. Black, I. Dodd, M.M. Harding, S.J. Winkley, J. Chem. Soc., Dalton Trans. (1993) 709.
[42] N.V. Gerbeleu, V.B. Arion, J. Burgess, Template Synthesis of Macrocyclic Compounds, Wiley-VCH, Weinheim, 1999.
[43] S. Akine, S. Sunaga, T. Taniguchi, H. Miyazaki, T. Nabeshima, Inorg. Chem. 46 (2007 2959).
[44] N.E. Borisova, M.D. Reshetova, Y.A. Ustynyuk, Chem. Rev. 107 (2007) 46.
[45] A.J. Gallant, J.K.-H. Hui, F.E. Zahariev, Y.A. Wang, M.J. MacLachlan, J. Org. Chem. 70 (2005) 7936.
[46] T. Nabeshima, H. Miyazaki, A. Iwasaki, S. Akine, T. Saiki, C. Ikeda, Tetrahedron 63 (2007) 3328.
[47] T. Nabeshima, H. Miyazaki, A. Iwasaki, S. Akine, Chem. Lett. 35 (2006) 1070.
[48] A.J. Gallant, B.O. Patrick, M.J. MacLachlan, J. Org. Chem. 69 (2004) 8739.
[49] S. Akine, T. Taniguchi, W. Dong, S. Masubuchi, T. Nabeshima, J. Org. Chem. 70 (2005) 1704.
[50] R. Atkins, G. Brewer, E. Kokot, G.M. Mockler, E. Sinn, Inorg. Chem. 24 (1985) 127.
[51] A.J. Gallant, J.H. Chong, M.J. MacLachlan, Inorg. Chem. 104 (2006) 697.
[52] P.D. Frischmann, A.J. Gallant, J.H. Chong, M.J. MacLachlan, Inorg. Chem. 47 (2008) 101.
[53] P.D. Frischmann, M.J. MacLachlan, Chem. Commun. (2007) 4480.
[54] P.D. Frischmann, M.J. MacLachlan, Comments Inorg. Chem. 29 (2008) 26.
[55] F.H. Allen, Acta Crystallogr., Sec. B 58 (2002) 380.